

Synthesis and Antisense Properties of Fluoro Cyclohexenyl Nucleic Acid (F-CeNA), a Nuclease Stable Mimic of 2'-Fluoro RNA

Punit P. Seth,^{†,*} Jinghua Yu,[†] Ali Jazayeri,[†] Pradeep S. Pallan,[‡] Charles R Allerson,[§] Michael E. Østergaard,[†] Fengwu Liu,^{||} Piet Herdewijn,^{||} Martin Egli,[‡] and Eric E. Swayze[†]

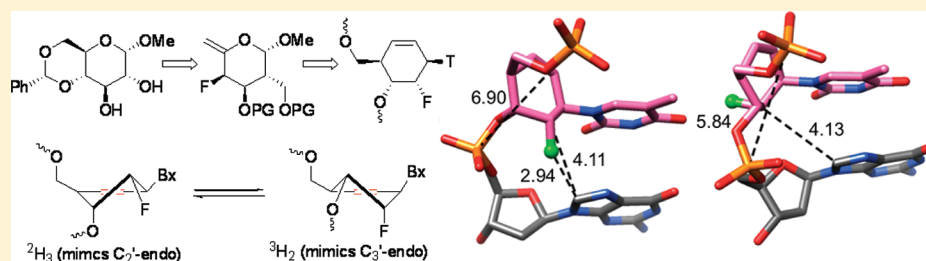
[†]Isis Pharmaceuticals, 2855 Gazelle Court, Carlsbad, California 92010, United States

[‡]Department of Biochemistry, School of Medicine, Vanderbilt University, 607 Light Hall, Nashville, Tennessee 37232, United States

[§]Regulus Therapeutics, 3545 John Hopkins Ct., San Diego, California 92121, United States

^{||}Laboratory of Medicinal Chemistry, Rega Institute for Medical Research, Katholieke Universiteit, Minderbroedersstraat 10, 3000 Leuven, Belgium

S Supporting Information



ABSTRACT: We report the design and synthesis of 2'-fluoro cyclohexenyl nucleic acid (F-CeNA) pyrimidine phosphoramidites and the synthesis and biophysical, structural, and biological evaluation of modified oligonucleotides. The synthesis of the nucleoside phosphoramidites was accomplished in multigram quantities starting from commercially available methyl-D-mannose pyranoside. Installation of the fluorine atom was accomplished using nonafluorobutanesulfonyl fluoride, and the cyclohexenyl ring system was installed by means of a palladium-catalyzed Ferrier rearrangement. Installation of the nucleobase was carried out under Mitsunobu conditions followed by standard protecting group manipulations to provide the desired pyrimidine phosphoramidites. Biophysical evaluation indicated that F-CeNA shows behavior similar to that of a 2'-modified nucleotide, and duplexes with RNA showed slightly lower duplex thermostability as compared to that of the more rigid 3'-fluoro hexitol nucleic acid (FHNA). However, F-CeNA modified oligonucleotides were significantly more stable against digestion by snake venom phosphodiesterases (SVPD) as compared to unmodified DNA, 2'-fluoro RNA (FRNA), 2'-methoxyethyl RNA (MOE), and FHNA modified oligonucleotides. Examination of crystal structures of a modified DNA heptamer duplex d(GCG)-T*-d(GCG):d(CGACGCG) by X-ray crystallography indicated that the cyclohexenyl ring system exhibits both the ³H₂ and ²H₃ conformations, similar to the C3'-endo/C2'-endo conformation equilibrium seen in natural furanose nucleosides. In the ²H₃ conformation, the equatorial fluorine engages in a relatively close contact with C8 (2.94 Å) of the 3'-adjacent dG nucleotide that may represent a pseudo hydrogen bond. In contrast, the cyclohexenyl ring of F-CeNA was found to exist exclusively in the ³H₂ (C3'-endo like) conformation in the crystal structure of the modified A-form DNA decamer duplex [d(GCGTA)-T*-d(ACGC)]₂. In an animal experiment, a 16-mer F-CeNA gapmer ASO showed similar RNA affinity but significantly improved activity compared to that of a sequence matched MOE ASO, thus establishing F-CeNA as a useful modification for antisense applications.

INTRODUCTION

The 2'-deoxy-2'-fluoro modification of RNA (FRNA 3, Figure 1) has been extensively investigated in the context of antisense therapeutics. FRNA modified nucleic acids have been used for RNase H based antisense,¹ as ribozymes,² as modulators of RNA splicing,³ as microRNA antagonists,⁴ for chemically modifying the sense and antisense strands in siRNA duplexes,^{5,6} as well as for improving the properties of oligonucleotide aptamers. Macugen (pegaptanib), a FRNA modified oligonucleotide aptamer targeting vascular endothelial growth factor

(VEGF), has been approved by the FDA for treatment of macular degeneration.⁷

FRNA modified oligodeoxyribonucleotides show improved duplex thermal stability when paired with RNA strands and also show improved stability toward nuclease-mediated degradation relative to unmodified oligonucleotides.^{8,9} The electronegative nature of fluorine in FRNA causes the nucleoside furanose ring to adopt the C3'-endo sugar pucker and modified duplexes with

Received: March 21, 2012

Published: May 15, 2012

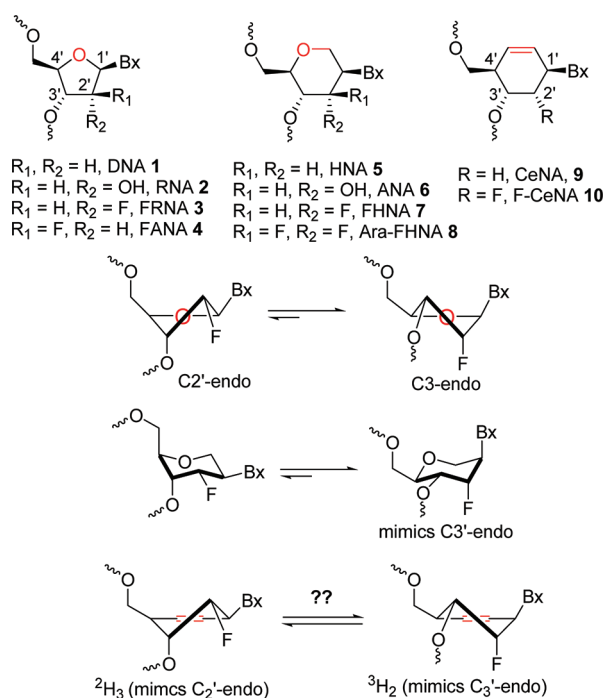


Figure 1. Structures of nucleic acid modifications and conformational equilibrium of the furanose, hexitol, and cyclohexene ring in FRNA, FHNA, and F-CeNA, respectively.

RNA resemble the A-type helical geometries reminiscent of RNA/RNA duplexes.¹⁰ However, unlike RNA/RNA duplexes where the 2'-hydroxyl group participates extensively in hydrogen-bonding with the water of hydration lattice around the sugar–phosphate backbone in the minor groove, the 2'-fluorine does not participate in hydrogen bonding with the water lattice.¹¹ As a result, FRNA modified duplexes have a considerably drier minor groove, and the improved duplex thermal stability has been attributed to increased enthalpy as a result of stronger Watson–Crick base pairing.¹¹

To further explore the impact of fluorination on the biophysical and biological properties of nucleic acids, a number of other fluorinated nucleic acids analogues have been reported in the literature (Figure 1). Some notable examples include the “arabino” configured fluorinated analogue of DNA (FANA **4**), which improves the thermal stability of oligonucleotide duplexes and is one of a handful of analogues that support cleavage of modified duplexes by RNase H.^{12–15} However, in the case of FANA, the improved duplex thermostability stems from formation of a pseudo H...F bond between H-8 on the purine nucleobases and the 2'-fluorine atom in the “arabino” configuration on the 5'-adjacent nucleotide at purine-pyrimidine steps.¹⁶ In addition, we have also recently reported the synthesis and antisense properties of both isomers of 3'-fluoro hexitol nucleic acid (FHNA **7** and Ara-FHNA **8**),¹⁷ as well as the R- and S-6'-Me backbone modifications of FHNA.¹⁸ Hexitol nucleic acid (HNA **5**) modified oligodeoxyribonucleotides, first described by the Herdewijn group, show improved affinity for complementary RNA.¹⁹ In the hexitol series, the relatively flexible furanose ring found in DNA and RNA is replaced with a more rigid six-membered hexitol ring and the position of the nucleobase is moved from the anomeric carbon to the 3'-position. This arrangement presents the nucleobase in an axial orientation and as such mimics the C3'-endo sugar pucker.²⁰ Our studies showed that the HNA analogue with the

axial fluorine atom (FHNA) improved oligonucleotide duplex thermal stability when paired with RNA, whereas the analogue with the equatorial fluorine atom (Ara-FHNA) was destabilizing. These observations were further rationalized using structural data.¹⁷ FHNA modified gapmer phosphorothioate antisense oligonucleotides (ASOs) also showed excellent activity in animal experiments that was comparable to the activity observed with the corresponding sequence matched LNA ASOs despite a lower overall T_m . The improved activity of FHNA ASOs was attributed to a more efficient functional uptake of the fluorinated ASO into liver tissue.¹⁷

The Herdewijn group has also introduced another series of nucleic acid analogues where the hexitol ring was replaced with a cyclohexenyl ring system (CeNA).^{21–24} The cyclohexenyl ring is conformationally more flexible as compared to the hexitol ring, and the two extreme half-chair conformations of CeNA (2H_3 and 3H_2) resemble the conformational states of the C2'-endo and C3'-endo sugar puckers of the furanose ring in DNA and RNA. Structural studies showed that the ring conformation adopted by CeNA nucleotides within a modified oligonucleotide duplex is dependent on the overall helical geometry of the duplex. For example, CeNA nucleotides were found to exist in the 3H_2 conformation (similar to C3'-endo sugar pucker) in a fully modified octamer GTGTACAC,²⁵ while the cyclohexene ring was found to adopt the 2E -conformation when placed in the center of the Dickerson dodecamer GCGCAATTTCGCG.²⁶ In another study CeNA was found to adopt both the 2H_3 and the 3H_2 conformations in B-type helices when incorporated into a non-self complementary sequence GCGTGC.²⁷ CeNA substitution into the sense or antisense strand was found to improve the activity of modified siRNA duplexes in cell culture experiments.²⁸ Further structural and modeling studies using the CeNA modified siRNA showed that the CeNA/RNA duplex bound to the PIWI protein did not show major differences in interactions between the protein and the CeNA modified antisense strand as compared to an unmodified RNA/RNA duplex.²⁸

Given the interesting structural and biological properties of CeNA and various fluorinated nucleic acid analogues and the observation that unsaturated moieties can serve as bioisosters for an oxygen atom in nucleic acid structures,²⁹ we were keen on assessing the biophysical and biological properties of 2'-fluoro CeNA (F-CeNA) as a modification for antisense therapeutics. It is conceivable that fluorine substitution could further improve the hybridization properties of CeNA modified oligonucleotides by increasing the strength of Watson–Crick base pairing or by biasing the cyclohexenyl ring toward the 3H_2 pucker by participating in nonbonding interactions with the π system of the cyclohexenyl ring. In addition, inserting fluorine into the already less hydrated minor groove of CeNA duplexes with RNA could have an impact on the biological properties of modified oligonucleotides since the minor groove is an important recognition element for proteins such as RNase H^{30,31} and Ago-2,³² which mediate antisense effects.

To address these issues, we synthesized both of the pyrimidine nucleoside phosphoramidites of F-CeNA in multi-gram quantities and characterized the biophysical and biological properties of F-CeNA modified oligodeoxyribonucleotides in T_m , nuclease stability and animal experiments. In this report, we show that F-CeNA substitution is well tolerated and the modified oligonucleotides show equivalent duplex stabilizing properties relative to FRNA and CeNA but not FHNA when paired versus RNA complements and a greatly enhanced

nuclease stability profile relative to FRNA and FHNA modified oligonucleotides. In an animal experiment, a F-CeNA phosphorothioate modified gapmer oligonucleotide showed significantly improved potency as compared to a sequence matched MOE counterpart, thus establishing F-CeNA as a useful modification for antisense applications.

RESULTS AND DISCUSSION

The Herdewijn group has described a number of methods for the synthesis of CeNA nucleosides.^{22,24,33–35} We envisaged that F-CeNA nucleosides could be prepared in an enantio-controlled manner by using the general strategy described for the preparation of Ara-CeNA nucleosides.³⁶ This strategy was adapted from the total synthesis of cyclophellitol originally described by Jung.³⁷ Retrosynthetically, the DMTr protected F-CeNA phosphoramidite **11** could be prepared by appropriate protecting group manipulations from a suitably protected F-CeNA monomer **12**, which in turn could be accessed from the allylic alcohol **13** by means of a Mitsunobu reaction (Figure 2).

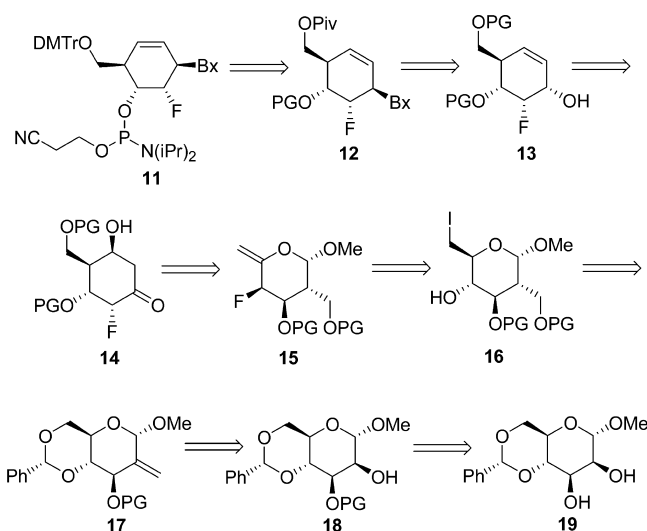


Figure 2. Retrosynthesis of F-CeNA phosphoramidite.

Allylic alcohol **13** was anticipated from the beta-hydroxy ketone **14** by elimination of the beta hydroxyl group followed by a Luche reduction of the intermediate enone. Ketone **14** could in turn be prepared from sugar **15** by means of a Ferrier rearrangement. The exocyclic double bond in **15** could be installed by elimination of the 6'-iodo atom in **16** while the fluorine atom could be introduced by an S_N2 inversion of the 4'-hydroxyl group. The 2'-hydroxymethyl group in **16** could arise by hydroboration of the exocyclic double bond in **17**, which in turn could be installed by means of a Wittig reaction on the 3'-protected benzylidene **18**. Lastly, **18** could be prepared by selective protection of the known sugar intermediate **19**.

Synthesis of the F-CeNA monomer was initiated from the known methyl-mannopyranosyl benzylidene protected sugar **19** (Scheme 1). Selective protection of the equatorial 3'-hydroxyl group as the Nap ether^{38,39} was accomplished by alkylation of the cyclic stannylidene ether with 2-bromomethylnaphthalene to provide **20**. Oxidation of the primary alcohol using the Swern conditions followed by a Wittig olefination provided the exocyclic olefin **21**. Hydroboration of the olefin using 9-BBN followed by oxidation of the intermediate boronate species with

sodium perborate provided the 2'-hydroxymethyl sugar **22** as a mixture of diastereoisomers. Equilibration of the mixture to give the more stable equatorial hydroxymethyl diastereoisomer was accomplished by a three-step process.³⁷ The primary hydroxyl group was first oxidized to the aldehyde using the Swern conditions⁴⁰ followed by treatment with triethylamine to yield the equatorial aldehyde and subsequent reduction with sodium borohydride to provide **23**. Protection of the primary hydroxyl group as the pivaloyl (Piv) ester followed by opening of the benzylidene ring using aqueous HCl provided the diol **24** in good yield. We found that it was not necessary to protect the secondary 4'-hydroxyl group for selective conversion of the primary 6'-hydroxyl group to the iodide **25**. Gratifyingly, fluorination of the secondary equatorial 4'-hydroxyl group to the axial fluoride **26** proceeded smoothly using DBU and nonafluorobutanesulfonyl fluoride as the fluorinating agent.⁴¹ Attempts to eliminate the 6'-iodide in **26** using DBU as reported previously resulted in variable results. The major byproduct of this reaction, as indicated by LC-MS analysis of the crude reaction mixtures, appeared to be adducts arising from nucleophilic displacement of the iodide with DBU. Instead, this elimination was carried out using silver fluoride in DMF⁴² to provide the exocyclic olefin **27** in essentially quantitative yield. While the Ferrier rearrangement of **27** to the carbocycle **28** could be carried out using $HgCl_2$,³⁷ we found that this transformation could also be effected equally efficiently using catalytic $PdCl_2$.⁴³ Mesylation of the hydroxyl group and subsequent elimination to the enone **29** was carried out in good yield using methanesulfonyl chloride in pyridine on a gram scale. Unfortunately, during the scale-up effort, attempts to remove portion of the pyridine on a rotary evaporator prior to aqueous workup resulted in the formation of a large amount of **30**, presumably due to deprotonation of the acidic γ proton followed by elimination of the adjacent pivaloxy group.⁴⁴ Despite this setback, we were still able to prepare >12 g of **31** for completing the synthesis of the pyrimidine monomer phosphoramidites. While the mesylation/elimination sequence was not attempted at scale again, we believe that this problem can be avoided by using a solvent other than pyridine for the reaction or by extracting the hydrophobic enone **29** into ethyl acetate followed by aqueous washes to remove pyridine from the product prior to concentration. Reduction of the enone under Luche conditions⁴⁵ provided the allylic alcohol **31** with axial attack of the hydride nucleophile onto the carbonyl group.

Synthesis of the protected thymine nucleobase monomer **33** was accomplished by means of a Mitsunobu reaction between **31** and N3-benzoyl protected thymine. The use of the protected nucleobase was necessary to avoid reaction at the more acidic N3-position. We also detected formation of a second byproduct from this reaction **34** arising from reaction at O2 of N3-benzoyl protected thymine. Removal of the Nap protecting group in **33** with DDQ³⁹ followed by deprotection of the pivaloyl and the N3-benzoyl groups with potassium carbonate in methanol provided the unprotected thymine monomer **35**. The identity and absolute stereochemistry of **35** was unambiguously assigned by X-ray crystallography (Figure 3). Protection of the primary alcohol in **35** as the DMTr ether to give **36** followed by a phosphitylation reaction provided the phosphoramidite **37**, which was now ready for solid-phase oligonucleotide synthesis.

Synthesis of the N4-benzoyl protected cytosine monomer was accomplished using a procedure described previously (Scheme 2).³⁹ Protection of the secondary hydroxyl group in

Scheme 1. Synthesis of F-CeNA Thymine Phosphoramidite

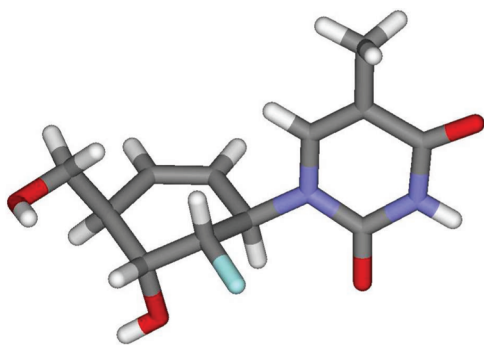
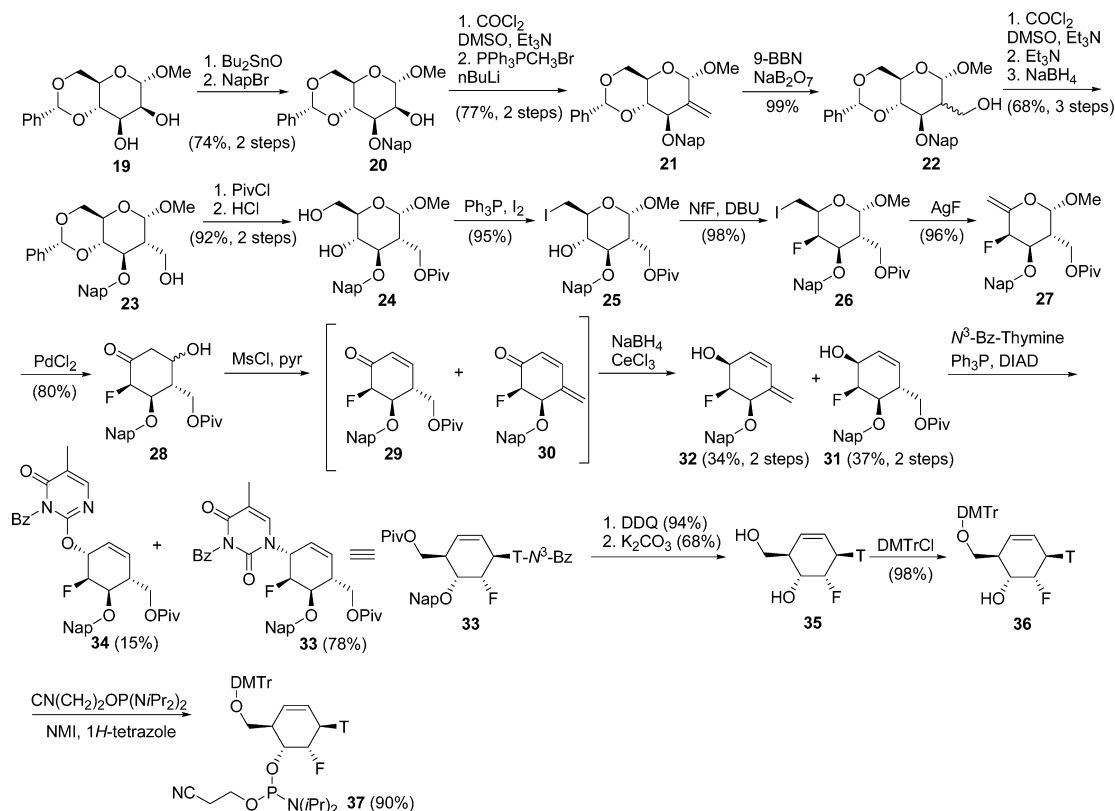
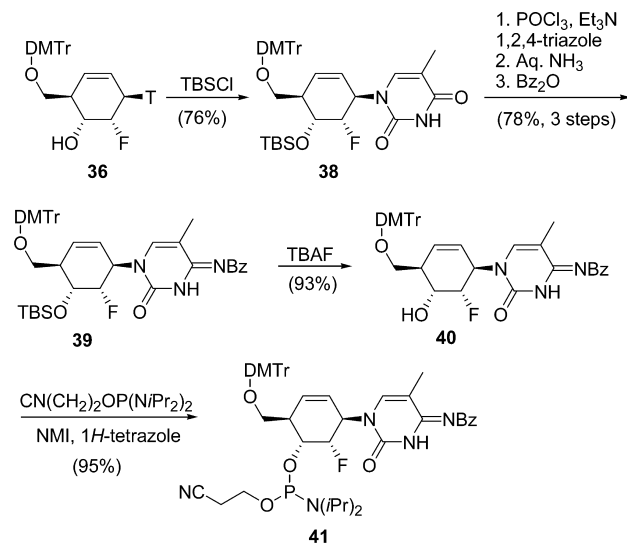


Figure 3. X-ray crystal structure of F-CeNA thymine monomer 35.

36 as the TBS ether to provide 38 followed by a three-step sequence (C4-triazolide formation, displacement with ammonia, and benzylation of exocyclic amino group) provided the N4-benzoyl cytosine monomer 39.⁴⁶ Removal of the TBS group to provide 40 followed by a phosphorylation reaction provided the desired phosphoramidite 41.

Synthesis of F-CeNA modified oligodeoxyribonucleotides was accomplished using standard phosphoramidite chemistry on an automated DNA synthesizer. Oligonucleotides were synthesized at 2 micromole scale on polystyrene resin using DCI as the activator and iodine/water as the oxidizing agent.³⁹ A coupling time of 5 min was used for the F-CeNA monomers, and the average yield for incorporation was >95%. Cleavage of the oligonucleotides from the resin as well as deblocking of the base protecting groups was accomplished by heating the resin in aqueous ammonia after completion of the synthesis. The crude oligonucleotides were purified by ion exchange

Scheme 2. Synthesis of F-CeNA 5-Methyl Cytosine Phosphoramidite



chromatography followed by desalting on reverse phase to provide the final oligonucleotides.

The modified oligonucleotides were evaluated in T_m experiments to ascertain the effect of F-CeNA incorporation on duplex thermal stability when paired with RNA complements (Table 1). We used two different sequences for the T_m measurements. In the first sequence we examined the effect of one, two, and three tandem incorporations of F-CeNA in the middle of a stretch of dT nucleotides (5'-d-(GCGTTTTTTTGCT)-3', 5'-d-(GCGTTTTTTTGCT)-3', and 5'-d-(GCGTTTTTTTGCT)-3' where the modified nucleotide is

Table 1. Duplex Thermal Stability (T_m) Measurements of MOE, FRNA, FHNA, F-CeNA, and CeNA Modified DNA Containing One, Two, or Three Modified Nucleotides versus RNA Complements

sequence ^a	$\Delta T_m/\text{modification } (^{\circ}\text{C})^b$				
	MOE	FRNA	FHNA	F-CeNA	CeNA
5'-d(GCGT <u>TT</u> TTTGCT)-3'	-2.2	-0.6	+0.6 ^c	-1.8	-0.6
5'-d(GCGT <u>TT</u> TTTGCT)-3'	+0.2	+0.1	+1.7 ^c	-0.2	+0.3
5'-d(GCGT <u>TT</u> TTTGCT)-3'	+0.3		+1.7	+0.1	+0.5
5'-d(CCAGT <u>GAT</u> ATGC)-3'	+1.8	+1.8	+2.6 ^c	+1.7	+1.0

^aUppercase letters indicate 2'-deoxynucleotides, and bold underlined letters indicate modified nucleotides. ^b T_m values were measured at 4 μM oligo concentration in 10 mM sodium phosphate buffer (pH 7.2) containing 100 mM NaCl and 0.1 mM EDTA; the sequences of the RNA complements were 5'-r(AGCAAAAACGC)-3' and 5'-r(GCAUAUCACUGG)-3'; ^cReference 17.

bold and underlined). We also prepared the corresponding MOE, FRNA, FHNA, and CeNA modified oligonucleotides as controls. Somewhat surprisingly, a single incorporation of MOE, FRNA, CeNA, or F-CeNA in the middle of a stretch of dT nucleotides reduced duplex thermal stability, two incorporations were T_m neutral, and three incorporations were stabilizing relative to unmodified DNA. In contrast, a single incorporation of FHNA in which the hexitol ring mimics the C3'-endo (N-type) sugar pucker, was slightly stabilizing, whereas two and three incorporations had a significant stabilizing effect on duplex thermostability. We and others have previously examined the duplex stabilizing properties of several 2',4'-bridged nucleic acids (BNA, also known as locked nucleic acids or LNA) analogues in this sequence, and a single incorporation of a BNA nucleotide typically produces a +5 $^{\circ}\text{C}$ enhancement in duplex thermal stability when paired with DNA or RNA complements.^{29,39,47-53} It is known that insertion of BNA nucleotides into DNA results in conformational tuning of the adjacent 2'-deoxynucleotides toward the C3'-endo conformation.⁵⁴ It is likely that this occurs more efficiently with BNA nucleotides as compared to the more flexible 2'-modified nucleotides or the relatively less flexible (but not locked) hexitol nucleic acids. Thus, one could rationalize that a single incorporation of MOE, FRNA, CeNA, or F-CeNA in a stretch of dTs produces a local destabilizing change in the oligonucleotide duplex resulting in a slight decrease in T_m . In contrast, two or more incorporations of these nucleotides starts to change the overall duplex conformation toward a more stable A-type helical geometry resulting in a net stabilizing effect on duplex thermostability.

We also evaluated the duplex stabilizing properties of all of the above modifications in a second sequence (5'-d(CCAGT**GAT**ATGC)-3', modified nucleotide is bold and underlined) using three incorporations of the modified nucleotides. An important difference here was that the modified nucleotides are now flanked by purine deoxynucleotides, thus providing a different sequence context for the T_m evaluation. In this sequence, F-CeNA, MOE, and FRNA showed good duplex stabilizing properties (ΔT_m +1.8 $^{\circ}\text{C}/\text{mod}$), while CeNA was slightly less stabilizing (ΔT_m +1.0 $^{\circ}\text{C}/\text{mod}$). However, F-CeNA was still less stabilizing as compared to FHNA by ~ 1 $^{\circ}\text{C}/\text{mod}$.¹⁷ Thus the T_m data suggests that F-CeNA does not produce a dramatic increase in RNA-affinity relative to that of CeNA and behaves more like FRNA as opposed to FHNA

when paired with RNA complements. The data also suggests that F-CeNA retains the conformational flexibility characteristic of furanose nucleotides in contrast to FHNA, where the more rigid hexitol ring exists predominantly in the C3'-endo sugar pucker.

We next evaluated the ability of F-CeNA to stabilize DNA against 3'-exonuclease digestion using snake venom phosphodiesterase (SVPD) (Table 2). We prepared 12-mer poly-T

Table 2. 3'-Exonuclease Stability of the Phosphosphodiester Linkage in DNA, MOE, FRNA, F-CeNA, and FHNA Modified Oligonucleotides

sequence	modification ^a	$T_{1/2}$ (min) ^b
5'-d(TTTTTTTTT <u>TT</u>)-3'	DNA	0.23
5'-d(TTTTTTTTT <u>TT</u>)-3'	MOE	4.3
5'-d(TTTTTTTTT <u>TT</u>)-3'	FRNA	1.64
5'-d(TTTTTTTTT <u>TT</u>)-3'	F-CeNA	>24 h
5'-d(TTTTTTTTT <u>TT</u>)-3'	FHNA	160

^aUppercase letters indicate 2'-deoxynucleotides, and bold underlined letters indicate modified nucleotides. ^bEach oligonucleotide was prepared as a 500 μL mixture containing 12.5 μL of 200 μM oligomer, 50 μL of SVPD at 0.005 U/mL in SVPD buffer (50 mM Tris-HCl, pH 7.5, 8 mM MgCl₂) final concentration 0.0005 U/mL, and 438.5 μL of SVP buffer. Samples were incubated at 37 $^{\circ}\text{C}$ in a thermoblock. Aliquots (50 μL) were taken at different intervals. EDTA was added to aliquots immediately after removal to quench enzyme activity, and the samples were analyzed on IP HPLC-MS. The results are expressed as half-life ($T_{1/2}$) in minutes.

oligonucleotides containing 2 incorporations of the modified nucleotide at the 3'-terminus. In this study, the F-CeNA modified oligonucleotide was exceptionally stable with a half-life >24 h. In contrast, the FRNA and MOE modified oligonucleotides were completely degraded in <5 min while the FHNA modified oligo was more stable ($T_{1/2}$ = 160 min). We did not evaluate the exonuclease stability of CeNA in this study so it is difficult to ascertain if the dramatic improvement in nuclease stability was a consequence of the cyclohexenyl ring system or the added fluorine substitution. However, on the basis of the differences in exonuclease stability between FRNA, FHNA, and F-CeNA, one can conclude that the improved nuclease stability of F-CeNA is most likely a result of the cyclohexenyl ring system, which lacks the 4' ring oxygen atom. This further suggests that the 4'-oxygen atom is an important recognition element for cleavage of the oligonucleotides by SVPD and could be involved in chelating metal ions in the enzyme active site.⁵⁵

We analyzed the conformational properties of F-CeNA T (T^*) in the crystal structure of the modified B-form DNA heptamer duplex d(GCG)- T^* -d(GCG):d(CGCACGC) determined to 1.57 \AA resolution (PDB ID code 4F2X; see Supporting Information Table 2 for experimental details and Supporting Information Figures 1 and 2 for the quality of the electron density). Unlike the corresponding duplex with incorporated CeNA T that crystallizes in a tetragonal space group,²⁷ crystals of the F-CeNA modified duplex belong to orthorhombic space group $P2_12_12_1$. However, both crystal lattices feature two independent duplexes per asymmetric unit that exhibit slightly distorted B-form conformations (Supporting Information Figures 1 and 2).

The structure of the F-CeNA modified duplex reveals that the 3'-fluorine affects the local conformation only minimally relative to the corresponding region in the CeNA structure

(Figure 4). Interestingly, in one duplex both F-CeNA T and CeNA-T exhibit a ${}^2\text{H}_3$ -type pucker that mimics the 2'-

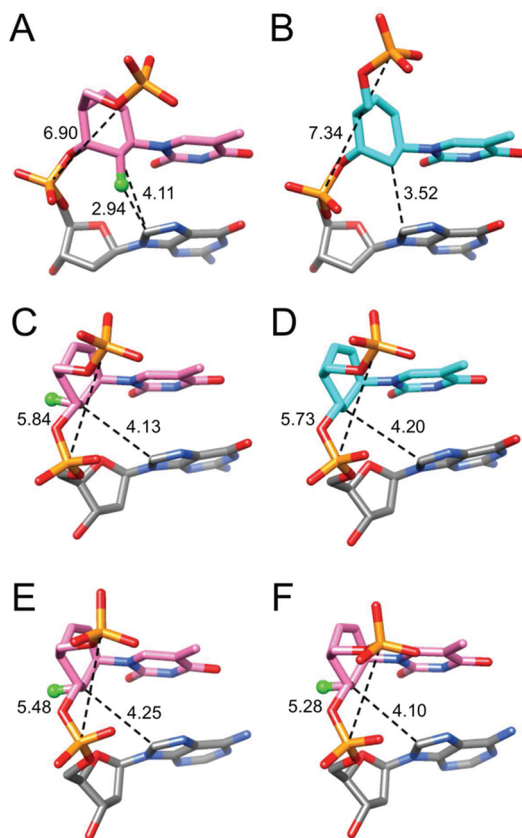


Figure 4. F-CeNA T exhibits conformational variations inside a B-form duplex and mimics the C3'-endo pucker inside an A-form duplex. (A) F-CeNA T with an equatorial orientation of 3'-fluorine that may result in the formation of a pseudo H-bond with C8-H from the adjacent guanine. (B) CeNA T in the structure of the DNA heptamer duplex of identical sequence adopts a very similar conformation.²⁷ (C) F-CeNA T in the second duplex with an axial orientation of 3'-fluorine and (D) the corresponding CeNA T adopting a very similar conformation. (E) F-CeNA T with an axial orientation of 3'-fluorine in the first strand and (F) in the second strand of the A-form DNA duplex. Carbon atoms of F-CeNA and CeNA Ts are colored in pink and cyan, respectively, F3' is highlighted as a green sphere, and P...P and C3'(T*)...C8(G) (and F3'...C8; panel A) separations are indicated by dashed lines with distances in Å.

deoxyribose C2'-endo state (Figure 4A and B, respectively). The B-form character of the backbone at the T*4pG5 step is also indicated by the relatively long P...P distance of 6.90 Å in the duplex containing F-CeNA T (7.34 Å, CeNA; nucleotides are numbered 1 to 7 in the GCGT*GCG heptamers). The equatorial orientation of fluorine leads to a slightly increased spacing between C3' of the cyclohexenyl ring and C8 from the adjacent guanine (Figure 4A and B). The fluorine engages in a relatively close contact with C8 (2.94 Å) that may represent a pseudo hydrogen bond,^{16,17} thus providing a rationalization for the considerably increased RNA affinity of DNAs with F-CeNA T incorporated at Py-Pu steps as opposed to being embedded within stretches of T (Table 1).

In the second duplex, F-CeNA T and CeNA T exhibit a ${}^3\text{H}_2$ -type pucker that mimics the ribose C3'-endo state (Figure 4C and D, respectively). The A-form character of the backbone at

the T*4pG5 step is indicated by a P...P distance of 5.84 Å in the duplex containing F-CeNA T (5.73 Å, CeNA). The fluorine with axial orientation juts into the minor groove and is not involved in any short intra- or internucleotide contacts (Figure 4C).

To assess the influence of the duplex form on the conformational preference of F-CeNA residues, we determined the crystal structure of the modified A-form DNA decamer duplex [d(GCGTA)-T*-d(ACGC)]₂ at 1.60 Å resolution (PDB ID code 4F2Y; see Supporting Information Table 2 for experimental details and Supporting Information Figures 3 and 4 for the quality of the electron density). Unlike in the B-form duplex, both F-CeNA Ts in the A-form duplex adopt a ${}^3\text{H}_2$ -type pucker that mimics the ribose C3'-endo state (Figure 4E and F). This observation supports the notion that an RNA environment shifts the F-CeNA conformational equilibrium toward the C3'-endo like state with an axial orientation of fluorine.

The structural data demonstrate that the presence of fluorine at the 3'-position of CeNA does not fundamentally alter the conformational flexibility of the cyclohexenyl moiety. Paired with RNA, F-CeNA-modifications within a DNA can be expected to increase the stability relative to the corresponding CeNA-DNA chimeric strand by pseudo H-bonding (an isolated F-CeNA residue) or by locking the cyclohexenyl ring in a C3'-endo mimicking conformation (consecutive stretch of F-CeNA residues).

Lastly, we evaluated the biological profile of F-CeNA using a 16-mer fully phosphorothioate (PS) modified gapmer antisense oligonucleotide (ASO) with a 10-base deoxynucleotide gap flanked on each end with three F-CeNA nucleotides (Table 3).

Table 3. T_m and in Vivo Activity of MOE and F-CeNA Gapmer ASOs Targeting Mouse PTEN mRNA

ASO ^a	T_m (°C) ^b	ED ₅₀ (mg/kg) ^c
MOE A1	62.4	91
F-CeNA A2	64.4	22

^aSequence used for evaluation: T^mCTTAGACTGGC^mCTT. Bold and underlined letters indicate modified residues in flanks, and uppercase letters indicate 2'-deoxynucleotides in the gap; all linkages are phosphorothioate modified. ^bSequence of 20-mer RNA complement used for T_m measurements: 5'-r-(UCAAGGCCAGUGCUAAGAGU)-3'. ^cPotency for PTEN mRNA reduction in mouse liver from single dose study.

This ASO targets mouse phosphatase and tensin homologue (PTEN) and represents a two nucleotide extension of a 14-mer sequence that we have previously used to profile the biological properties of multiple 2',4'-BNA and HNA analogues.^{17,56,57} We decided to use a slightly longer ASO sequence given that F-CeNA showed lower RNA affinity relative to that of FHNA and fortuitously, all of the modified nucleotides in the flanks needed pyrimidine nucleobases to maintain perfect complementarity to the PTEN mRNA. We included a sequence matched 16-mer MOE ASO as a control for the experiment. We first evaluated the duplex thermal stability of the modified ASOs versus a 20-mer RNA complement. Both the F-CeNA and MOE ASOs A1 and A2, respectively, showed almost identical duplex thermal stabilities thus corroborating our T_m observations from the earlier biophysical experiments.

In the animal experiment, mice (Balb-c, $n = 4$ /group) were injected subcutaneously with a single dose of 3.2, 10, 32, and

100 mg/kg of ASOs A1 and A2. The mice were sacrificed 48 h after ASO injection, the liver tissue was homogenized, and PTEN mRNA was quantified and normalized relative to the saline-treated group. The reductions in PTEN message were curve fitted using nonlinear regression software, and ED₅₀ values were calculated (Figure 5). Both ASOs were well

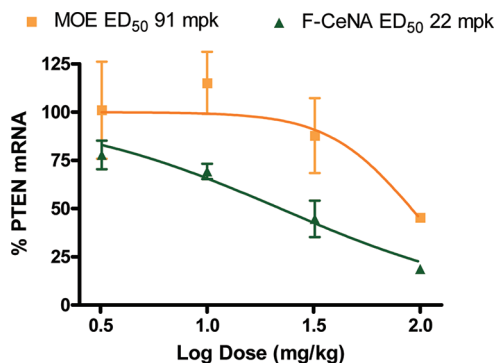


Figure 5. Dose–response curves for reducing PTEN mRNA using MOE and F-CeNA ASOs A1 and A2, respectively.

tolerated, but the F-CeNA ASO A2 (ED₅₀ = 22 mg/kg) showed almost 4-fold better activity than the MOE ASO A1 (ED₅₀ = 91 mg/kg) in the single dose–response experiment. This large difference in activity with the fluorinated ASO is consistent with our previous observations with a FHNA modified ASO that showed excellent activity in animals despite a lower overall T_m as compared to a sequence matched LNA benchmark ASO. However, it should be noted that the poor activity observed with the MOE ASO is not typical of second generation MOE ASOs, which are usually longer and have higher MOE content.

In conclusion, we report the design and synthesis of F-CeNA pyrimidine nucleoside phosphoramidites and the synthesis and biophysical, structural, and biological evaluation of modified oligonucleotides. The synthesis of the nucleoside phosphoramidites was accomplished in multigram quantities starting from commercially available and inexpensive methyl-D-mannose pyranoside. Elimination of the primary iodide was carried out very efficiently using AgF as opposed to DBU, which gave lower yields. Installation of the fluorine atom was accomplished using nonafluorobutanesulfonyl fluoride, and the cyclohexenyl ring system was assembled by means of a Ferrier rearrangement catalyzed by PdCl₂. The presence of a fluorine atom adjacent to the exocyclic enol ether did not impede or interfere with the Ferrier rearrangement process. Unfortunately, elimination of the pivaloyloxy group was observed during the scaleup process, but this can be easily avoided by carrying out the mesylation reaction in a solvent other than pyridine or by using an aqueous workup to extract **30** (as opposed to removing pyridine on a rotary evaporator). Installation of the nucleobase was carried out under Mitsunobu conditions followed by standard protecting group manipulations to provide the desired pyrimidine phosphoramidites.

Our biophysical studies with F-CeNA modified oligonucleotides suggest that fluorination provides a modest improvement in RNA affinity relative to CeNA. Overall, F-CeNA was found to behave like a typical 2'-modified nucleotide in the T_m experiments, and duplexes with RNA showed lower duplex thermostability as compared to that of the more rigid FHNA. F-CeNA modified oligonucleotides also showed a very dramatic

increase in stability against digestion by 3'-exonucleases. However, the improved nuclease stability could very well be a function of the cyclohexenyl ring system, which lacks the 4' ring oxygen atom. Examination of crystal structures of a modified DNA heptamer duplex d(GCG)-T*-d(GCG):d(CGACGC) by X-ray crystallography indicated that the cyclohexenyl ring system exhibits both the ³H₂ and ²H₃ conformations, similar to the C3'-endo/C2'-endo conformation equilibrium seen in natural furanose nucleosides. In the ³H₂ conformation, the equatorial fluorine engages in a relatively close contact with C8 (2.94 Å) of the 3'-adjacent dG nucleotide that may represent a pseudo hydrogen bond. In contrast, the cyclohexenyl ring of F-CeNA was found to exist exclusively in the ³H₂ (C3'-endo like) conformation in the crystal structure of the modified A-form DNA decamer duplex [d(GCGTA)-T*-d(ACGC)]₂. The structural data demonstrate that the presence of fluorine at the 3'-position of CeNA does not fundamentally alter the conformational flexibility of the cyclohexenyl moiety. Paired with RNA, F-CeNA modifications within a DNA can be expected to increase the stability relative to the corresponding CeNA-DNA chimeric strand by pseudo H-bonding (an isolated F-CeNA residue) or by locking the cyclohexenyl ring in a C3'-endo mimicking conformation (consecutive stretch of F-CeNA residues).

A F-CeNA gapmer ASO also showed similar RNA affinity as compared to that of a sequence matched MOE ASO but was significantly more active in the animal experiment. This observation is consistent with our previous results where a FHNA modified ASO showed improved activity in animal models relative to its sequence matched HNA counterpart despite similar overall T_m and activity in cell culture. While we only investigated F-CeNA in the context of RNase H antisense, it would be reasonable to expect that F-CeNA could be used as a nuclease stable surrogate in lieu of FRNA for other antisense applications. For example, Manoharan recently showed that FRNA modified siRNAs display unique gene silencing properties in animals,⁶ and the Herdewijn group has shown that CeNA modified siRNAs show good activity in cell culture.²³ Thus F-CeNA modified oligonucleotides could be used as a replacement for FRNA in RISC mediated gene silencing mechanisms or in oligonucleotide aptamers in addition to their utility for RNase H based antisense demonstrated in this report. In addition, F-CeNA could also find utility for the recently described “synthetic genetics” type applications, which use artificial nucleic acids for the storage and propagation of genetic information.⁵⁸

■ EXPERIMENTAL SECTION

Reagents were purchased from commercial vendors and used without any further purification. Unless stated otherwise, all reactions were carried out in oven-dried glassware that was capped with rubber septa and cooled to room temperature under an atmosphere of nitrogen. Animal experiments were carried out using the general procedures described previously.^{56,57}

Methyl 4,6-O-Benzylidene-3-O-(2-naphthyl-methyl)- α -D-mannopyranoside (20). A suspension of **19** (397 mmol, 112.0 g) prepared as previously described by Jung³³ and dibutyltin oxide (418 mmol, 104.0 g) in isopropanol (1100 mL) was refluxed until the solids dissolved (10 h). The solvent was then removed under reduced pressure to provide a white solid. 2-Bromomethyl naphthalene (757 mmol, 168.0 g) and CH₃CN (1100 mL) were added to the reaction flask, and the mixture was heated at 90 °C for 4 h. The reaction was cooled to room temperature and diluted with ethyl acetate. The organic layer was then washed with water and brine, dried (Na₂SO₄),

and concentrated. Purification by chromatography (silica gel, eluting with 25–40% ethyl acetate in hexanes) provided **20** (137.0 g, 74%). ¹H NMR (300 MHz, CDCl₃) δ: 7.86–7.77 (m, 3H), 7.76–7.68 (m, 1H), 7.55–7.43 (m, 5H), 7.42–7.34 (m, 3H), 5.64 (s, 1H), 4.99 (d, J = 12.1 Hz, 1H), 4.89 (d, J = 12.2 Hz, 1H), 4.77 (s, 1H), 4.28 (dd, J = 3.6, 9.0 Hz, 1H), 4.08 (d, J = 2.1 Hz, 1H), 3.95 (dd, J = 3.6, 9.6 Hz, 1H), 3.92–3.76 (m, 2H), 3.38–3.32 (m, 3H), 2.71 (s, 1H). ¹³C NMR (75 MHz, CDCl₃) δ: 137.6, 135.4, 133.3, 133.1, 129.0, 128.3, 128.0, 127.7, 126.6, 126.2, 126.0, 125.7, 101.7, 101.1, 78.8, 75.5, 72.9, 69.9, 68.9, 63.2, 55.0. HRMS-QTOF [M + H]⁺ calcd for C₂₅H₂₇O₆ 423.1808; found 423.1799. LRMS-ESI found 445.1.

Methyl 4,6-O-Benzylidene-2-deoxy-2-methylene-3-O-(2-naphthyl-methyl)-α-D-glucopyranoside (21). Dimethylsulfoxide (890 mmol, 63.0 mL) was added to a cold (–78 °C) solution of oxalyl chloride (440 mmol, 39.0 mL) in dichloromethane (700 mL). After stirring for 30 min a solution of **20** (136.0 g, 306.0 mmol) in dichloromethane (800 mL) was added to the reaction, and the stirring was continued for another 45 min. Triethylamine (1330 mmol, 187 mL) was then added to the reaction, and the cooling bath was removed. After another 30–45 min of stirring, TLC analysis indicated no more starting **20**. The reaction was then diluted with dichloromethane, and the organic layer was sequentially washed with 5% HCl, saturated sodium bicarbonate, and brine, dried (Na₂SO₄), and concentrated to provide the crude ketone (135.0 g), which was used without any further purification. ¹H NMR (300 MHz, CDCl₃) δ: 7.93–7.62 (m, 4H), 7.59–7.32 (m, 8H), 5.58 (s, 1H), 5.10 (d, J = 12.8 Hz, 1H), 4.86 (d, J = 12.6 Hz, 1H), 4.76 (s, 1H), 4.57 (d, J = 10.4 Hz, 1H), 4.38 (dd, J = 4.8, 10.3 Hz, 1H), 4.25–4.11 (m, 1H), 3.98–3.77 (m, 2H), 3.45 (s, 3H). LRMS-ESI [M + Na]⁺ calcd 443.2, found 443.1.

nBuLi (500 mmol, 200 mL of a 2.5 M solution) was added to a cold (0 °C) suspension of methyltriphenylphosphonium bromide (500 mmol, 179.0 g) in THF (800 mL). After stirring for 2 h, the temperature was lowered to –78 °C, and a solution of the crude ketone obtained above in THF (1000 mL) was added to the reaction, which was gradually allowed to warm to room temperature. After stirring for 16 h, the reaction was quenched with saturated ammonium chloride, and the mixture stirred for 30 min. The reaction was then diluted with ethyl acetate, and the organic layer was washed with water and brine, dried (Na₂SO₄), and concentrated. Purification by chromatography (silica gel, eluting with 10–20% ethyl acetate in hexanes) provided compound **21** (77 g, 58% from **20**). ¹H NMR (300 MHz, CDCl₃) δ: 7.88–7.75 (m, 3H), 7.74–7.66 (m, 1H), 7.54–7.38 (m, 8H), 5.61 (s, 1H), 5.54 (s, 1H), 5.24 (s, 1H), 5.08–5.04 (m, 1H), 5.03–4.91 (m, 2H), 4.52 (d, J = 9.4 Hz, 1H), 4.30 (dd, J = 4.9, 10.2 Hz, 1H), 4.02 (dt, J = 4.8, 9.7 Hz, 1H), 3.78 (t, J = 10.3 Hz, 1H), 3.69 (t, J = 9.6 Hz, 1H), 3.38 (s, 3H). ¹³C NMR (75 MHz, CDCl₃) δ: 142.4, 137.5, 135.9, 133.3, 133.0, 129.0, 128.3, 128.1, 128.0, 127.6, 126.2, 126.0, 125.8, 125.7, 112.9, 103.3, 101.4, 84.2, 76.7, 73.7, 69.1, 63.8, 54.6. HRMS-QTOF [M + Na]⁺ calcd for C₂₆H₂₆NaO₅ 441.1678; found 441.1667. LRMS-ESI found 441.1.

Methyl 4,6-O-Benzylidene-2-deoxy-2-C-β and α-hydroxy-methyl-3-O-(2-naphthyl-methyl)-α-D-glucopyranoside (22). 9-BBN (709 mmol, 1419 mL of a 0.5 M solution in THF) was added to a cold (0 °C) solution of **21** (177 mmol, 74.0 g) in THF (735 mL). The reaction was warmed to 40 °C and stirred for 16 h. The reaction was cooled in an ice-bath, carefully quenched with sodium hydroxide (3 N, 470 mL) and hydrogen peroxide (30% solution, 470 mL), and then stirred at room temperature for another 30 min. The reaction was diluted with ethyl acetate, and the organic layer was washed with water and brine, dried (Na₂SO₄), and concentrated. Purification by column chromatography (silica gel, eluting with 33% ethyl acetate in hexanes) provided **22** (78.0 g, 99%, contaminated with traces of 9-BBN byproducts). ¹H NMR (300 MHz, CDCl₃) δ: 7.90–7.66 (m, 8H), 7.59–7.30 (m, 17H), 5.64 (s, 2H), 5.10 (d, J = 11.3 Hz, 1H), 5.02–4.94 (m, 1H), 4.93–4.79 (m, 3H), 4.74 (s, 1H), 4.33–4.09 (m, 5H), 4.00–3.72 (m, 9H), 3.39 (s, 3H), 3.33 (s, 3H), 2.77 (d, J = 10.4 Hz, 1H), 2.64–2.45 (m, 2H), 2.17–1.98 (m, 1H). ¹³C NMR (75 MHz, CDCl₃) δ: 137.6, 135.9, 135.6, 133.3, 133.3, 133.0, 133.0, 129.0, 128.3, 128.3, 128.2, 128.0, 127.7, 126.9, 126.4, 126.2, 126.1, 126.1, 126.0,

125.9, 125.9, 125.6, 101.8, 101.7, 101.5, 101.0, 84.1, 80.2, 75.6, 75.1, 74.6, 73.6, 69.1, 63.4, 63.0, 61.1, 60.4, 55.0, 54.8, 47.5, 46.5, 22.7, 22.6. HRMS-QTOF [M + Na]⁺ calcd for C₂₆H₂₈NaO₆ 459.1784; found 459.1774. LRMS-ESI found 459.1.

Methyl 4,6-O-Benzylidene-2-deoxy-2-C-hydroxymethyl-3-O-(2-naphthyl-methyl)-α-D-glucopyranoside (23). Dimethylsulfoxide (510 mmol, 36.0 mL) was added to a cold (–78 °C) solution of oxalyl chloride (254 mmol, 22.0 mL) in dichloromethane (900 mL). After 30 min of stirring, a solution of **22** (182 mmol, 78.0 g) in dichloromethane (600 mL) was added to the reaction, and the stirring was continued for another 45 min. Triethylamine (760 mmol, 107.0 mL) was then added to the reaction, and the cooling bath was removed. After another 30–45 min of stirring, TLC analysis indicated no more starting **22**. The reaction was then diluted with dichloromethane, and the organic layer was sequentially washed with 5% HCl, saturated sodium bicarbonate, and brine, dried (Na₂SO₄), and concentrated to provide the crude aldehyde, which was used without any further purification. LRMS-ESI [M + Na]⁺ calcd 457.2, found 457.1.

A solution of the crude aldehyde from obtained above and triethylamine (228 mmol, 32.0 mL) in dichloromethane (1000 mL) was stirred for 5 days at room temperature. Sodium borohydride (182 mmol, 6.9 g) and methanol (200 mL) were added to the reaction, and the stirring was continued for 12 h at room temperature. The reaction was then concentrated on a rotary evaporator, and the residue was diluted with ethyl acetate. The organic layer was sequentially washed with 5% HCl, saturated sodium bicarbonate, and brine, dried, and concentrated. Purification by column chromatography (silica gel, eluting with 5–10% ethyl acetate in dichloromethane) provide the alcohol **23** (54 g, 68% from **22**). ¹H NMR (300 MHz, CDCl₃) δ: 7.85–7.72 (m, 4H), 7.56–7.35 (m, 8H), 5.64 (s, 1H), 5.10 (d, J = 11.3 Hz, 1H), 4.89 (d, J = 11.1 Hz, 1H), 4.81 (d, J = 3.6 Hz, 1H), 4.35–4.24 (m, 1H), 4.17 (dd, J = 8.5, 10.0 Hz, 1H), 3.94–3.75 (m, 5H), 3.41 (s, 3H), 2.81–2.69 (m, 1H), 2.11–2.01 (m, 1H). ¹³C NMR (75 MHz, CDCl₃) δ: 137.6, 135.9, 133.3, 133.0, 129.0, 128.3, 128.2, 128.0, 127.7, 126.9, 126.2, 126.1, 126.0, 125.8, 101.8, 101.5, 84.1, 75.1, 74.6, 69.1, 63.0, 60.5, 55.0, 47.5. HRMS-QTOF [M + Na]⁺ calcd for C₂₆H₂₈NaO₆ 459.1784; found 459.1775. LRMS-ESI found 459.1.

Methyl 2-Deoxy-3-O-(2-naphthyl-methyl)-2-C-pivaloyloxymethyl-α-D-glucopyranoside (24). Pivaloyl chloride (145 mmol, 17.6 mL) was added to a cold (0 °C) solution of **23** (120 mmol, 53.0 g), DMAP (12 mmol, 1.5 g), and triethylamine (240 mmol, 34.0 mL) in dichloromethane (1 L). The reaction was warmed to room temperature and stirred for 12 h. The reaction was carefully quenched with methanol (5 mL), and the organic phase was washed with 5% aqueous HCl, saturated sodium bicarbonate, and brine, dried (Na₂SO₄), and concentrated to provide the pivaloyl sugar (63.4 g, quantitative), which was used without any further purification. ¹H NMR (300 MHz, CDCl₃) δ: 7.91–7.68 (m, 4H), 7.59–7.34 (m, 9H), 5.64 (s, 1H), 5.06 (d, J = 11.3 Hz, 1H), 4.88–4.70 (m, 2H), 4.49 (dd, J = 4.0, 10.7 Hz, 1H), 4.29 (dd, J = 4.1, 9.5 Hz, 1H), 4.18–4.02 (m, 2H), 3.95–3.70 (m, 4H), 3.33 (s, 3H), 2.41–2.23 (m, 1H), 1.19 (s, 9H) LRMS-ESI [M + Na]⁺ calcd 543.2, found 543.2.

A solution of the pivaloyl sugar (120 mmol, 63.4 g) in a mixture of 1,4-dioxane (500 mL) and 1% HCl in methanol (500 mL) was heated at 45 °C for 3 h, after which it was cooled in an ice bath. A saturated solution of sodium bicarbonate (500 mL) was then carefully added to neutralize the acid, after which the organic solvent was removed on a rotary evaporator. The residue was extracted with dichloromethane, and the organic layer was washed with brine, dried (Na₂SO₄), and concentrated. Purification by column chromatography (silica gel, eluting with 25% ethyl acetate in hexanes followed by 5% MeOH in dichloromethane) provided **24** as a white foam (47.7 g, 92% from **23**). ¹H NMR (300 MHz, CDCl₃) δ: 7.88–7.78 (m, 4H), 7.53–7.44 (m, J = 9.2 Hz, 3H), 4.88 (s, 2H), 4.77 (d, J = 3.0 Hz, 1H), 4.49 (dd, J = 4.0, 10.7 Hz, 1H), 4.14 (t, J = 10.3 Hz, 1H), 3.82–3.79 (m, 2H), 3.74–3.61 (m, 3H), 3.33 (s, 3H), 2.59–2.52 (m, 1H), 2.29–2.16 (m, 1H), 2.09 (t, J = 6.3 Hz, 1H) 1.20 (s, 9H). ¹³C NMR (75 MHz, CDCl₃) δ: 178.2, 135.6, 133.3, 133.1, 128.6, 128.0, 127.8, 126.7, 126.3, 126.1, 125.7, 99.1, 78.9, 74.8, 72.2, 71.3, 62.7, 62.1, 55.2, 45.4, 38.9, 27.2.

HRMS-QTOF $[M + Na]^+$ calcd for $C_{24}H_{32}NaO_7$, 455.2046; found 455.2042. LRMS-ESI found 455.2.

Methyl 2,5-Dideoxy-5-iodo-3-O-(2-naphthyl-methyl)-2-C-pivaloyloxymethyl- α -D-glucopyranoside (25). A suspension of **24** (110 mmol, 47.5 g), triphenylphosphine (120 mmol, 31.8 g), imidazole (240 mmol, 16.5 g), and iodine (120 mmol, 31.0 g) in toluene (1 L) was heated at 50 °C for 1 h. The reaction was cooled to room temperature and quenched with saturated sodium thiosulfate. After stirring for 15 min, the reaction was diluted with ethyl acetate, and the organic layer was washed with brine, dried (Na_2SO_4), and concentrated. Purification by column chromatography (silica gel, eluting with 10–25% ethyl acetate in hexanes) provided **25** as a white foam (56.5 g, 95%). 1H NMR (300 MHz, $CDCl_3$) δ : 7.90–7.78 (m, 4H), 7.54–7.44 (m, 3H), 4.90 (d, $J = 11.5$ Hz, 1H), 4.86–4.75 (m, 2H), 4.49 (dd, $J = 4.0, 10.5$ Hz, 1H), 4.14 (t, $J = 10.3$ Hz, 1H), 3.69 (dd, $J = 8.1, 10.9$ Hz, 1H), 3.58–3.53 (m, 1H), 3.51–3.31 (m, 7H), 2.35–2.22 (m, 1H), 2.19 (d, $J = 3.2$ Hz, 1H), 1.20 (s, 9H). ^{13}C NMR (75 MHz, $CDCl_3$) δ : 178.1, 135.4, 133.3, 133.1, 128.7, 128.0, 127.8, 126.8, 126.4, 126.2, 125.6, 119.1, 78.8, 75.4, 74.8, 70.3, 62.0, 55.5, 45.5, 38.9, 27.2, 7.7. HRMS-QTOF $[M + Na]^+$ calcd for $C_{24}H_{31}INaO_6$, 565.1063, found 565.1055. LRMS-ESI found 565.0.

Methyl 2,4,5-Trideoxy-4-fluoro-5-iodo-3-O-(2-naphthyl-methyl)-2-C-pivaloyloxymethyl- α -D-galactopyranoside (26). Nonanfluorobutanesulfonyl fluoride (207 mmol, 38.6 mL) was added to a cold (0 °C) solution of **25** (103 mmol, 56.2 g) and DBU (207 mmol, 31.0 mL) in THF (1 L). The cooling bath was removed, and the reaction was stirred at room temperature for 2 h and then diluted with ethyl acetate (1 L). The organic layer was washed with 5% HCl, saturated sodium bicarbonate, and brine, dried (Na_2SO_4), and concentrated. Purification by chromatography (silica gel, eluting with 10% ethyl acetate in hexanes) provided **26** as a dark yellow gum (56.0 g, 98%). 1H NMR (300 MHz, $CDCl_3$) δ : 7.89–7.76 (m, 4H), 7.52–7.45 (m, 3H), 4.88 (d, $J = 51.3$ Hz, 1H), 4.87–4.82 (m, 2H), 4.70 (d, $J = 11.5$ Hz, 1H), 4.48 (dd, $J = 4.1, 10.7$ Hz, 1H), 4.08 (t, $J = 10.4$ Hz, 1H), 3.93–3.61 (m, 2H), 3.36 (s, 3H), 3.34–3.32 (m, 2H), 2.49–2.61 (m, 1H), 1.18 (s, 9H). ^{13}C NMR (75 MHz, $CDCl_3$) δ : 176.4, 133.0, 131.5, 126.8, 126.7, 126.2, 126.0, 125.0, 124.5, 124.4, 123.9, 97.5, 83.0 (d, $J = 185.3$ Hz, 1C), 71.2 (d, $J = 18.9$ Hz, 1C), 69.4, 68.3 (d, $J = 18.0$ Hz, 1C), 60.3, 54.0, 37.6 (d, $J = 1.5$ Hz, 1C), 37.1, 25.5. ^{19}F NMR (282 MHz, $CDCl_3$) δ : –220.9 (ddd, $J = 50.5, 27.5, 23.0$, 1F). HRMS-QTOF $[M + Na]^+$ calcd for $C_{24}H_{30}FINaO_5$, 567.1020, found 567.1013. LRMS-ESI found 567.1.

Methyl 2,4-Dideoxy-4-fluoro-3-O-(2-naphthyl-methyl)-2-C-pivaloyloxymethyl- α -D-psico-hex-5-enopyranoside (27). A solution of **26** (99.3 mmol, 54.1 g) and AgF (298 mmol, 38.0 g) in pyridine (1 L) was stirred in dark at room temperature for 3 days after which it was filtered through a Celite pad and washed with ethyl acetate. The resulting mixture was washed with water, 5% HCl, saturated sodium bicarbonate, and brine, dried (Na_2SO_4), and concentrated. Purification by chromatography (silica gel, eluting with 10% ethyl acetate in hexanes) provided **27** as a light yellow gum (39.7 g, 96%). 1H NMR (300 MHz, $CDCl_3$) δ : 7.89–7.77 (m, 4H), 7.49 (m, 3H), 5.08 (dd, $J = 2.1, 51.2$ Hz, 1H), 4.94 (d, $J = 2.8$ Hz, 1H), 4.91–4.81 (m, 2H), 4.77–4.66 (m, 2H), 4.50 (dd, $J = 4.1, 10.8$ Hz, 1H), 4.10 (t, $J = 10.3$ Hz, 1H), 3.96–3.75 (m, 1H), 3.35 (s, 3H), 2.86–2.73 (m, 1H), 1.19 (s, 9H). ^{13}C NMR (75 MHz, $CDCl_3$) δ : 178.1, 151.6 (d, $J = 7.5$ Hz, 1C), 134.9, 133.2, 133.2, 128.5, 128.0, 127.7, 126.7, 126.2, 126.1, 125.7, 103.2 (d, $J = 8.3$ Hz, 1C), 100.3, 85.2 (d, $J = 177.0$ Hz, 1C), 72.8 (d, $J = 20.3$ Hz, 1C), 71.3, 62.0, 55.7, 39.4 (d, $J = 2.3$ Hz, 1C), 38.8, 27.2. ^{19}F NMR (282 MHz, $CDCl_3$) δ : –189.9 (dd, $J = 53.6, 25.4$ Hz, 1F). HRMS-QTOF $[M + Na]^+$ calcd for $C_{24}H_{29}FNao_5$, 439.1897, found 439.1888. LRMS-ESI found 439.1.

(2R,3R,4S)-2-Fluoro-5-hydroxy-3-(methoxy-2-naphthalene)-4-(pivaloyloxymethyl)-cyclohexanone (28). A suspension of palladium(II) chloride (4.7 mmol, 0.83 g) and **27** (93.3 mmol, 38.9 g) in a 1,4-dioxane (600 mL) and water (300 mL) mixture was stirred at 70 °C for 20 min. The reaction was cooled to room temperature and extracted with ethyl acetate. The resulting solution was washed with brine, dried (Na_2SO_4), and concentrated. Purification by column chromatography (silica gel, eluting with 50% ethyl acetate in hexanes)

provided **28** as a clear gum (30.0 g, 80%). 1H NMR (300 MHz, $CDCl_3$) δ : 7.89–7.75 (m, 4H), 7.54–7.42 (m, 3H), 5.06 (d, $J = 51.0$ Hz, 1H), 4.88 (d, $J = 11.7$ Hz, 1H), 4.66 (d, $J = 11.7$ Hz, 1H), 4.51 (dd, $J = 8.7, 11.1$ Hz, 1H), 4.34 (dd, $J = 4.8, 11.4$ Hz, 1H), 4.24 (br. s., 1H), 3.96 (dd, $J = 23.4, 9.0$ Hz, 1H), 2.97 (td, $J = 4.1, 14.1$ Hz, 1H), 2.80 (br. s., 1H), 2.70–2.53 (m, 2H), 1.18 (s, 9H). ^{13}C NMR (75 MHz, $CDCl_3$) δ : 202.0 (d, $J = 19.5$ Hz, 1C), 179.5, 134.4, 133.2, 133.2, 128.5, 128.0, 127.7, 126.9, 126.3, 126.2, 125.7, 91.4 (d, $J = 185.3$), 75.7 (d, $J = 18.0$ Hz, 1C), 72.2, 65.5, 62.2, 44.5, 42.3 (d, $J = 3.8$ Hz, 1C), 38.9, 27.2. ^{19}F NMR (282 MHz, $CDCl_3$) δ : –201.5 (dd, $J = 51.6, 22.9$, 1F). HRMS-QTOF $[M + Na]^+$ calcd for $C_{23}H_{27}FNao_5$, 425.1740, found 425.1730. LRMS-ESI found 425.1.

(2S,3S,4R,5R)-3-Fluoro-2-hydroxy-4-(methoxy-2-naphthalene)-5-(pivaloyloxymethyl)-cyclohexene (31) and (2S,3S,4R)-3-Fluoro-2-hydroxy-4-(methoxy-2-naphthalene)-5-methylene-cyclohexene (32). Methanesulfonyl chloride (472 mmol, 37 mL) was added to a cold (0 °C) solution of **28** (94.5 mmol, 40.4 g) in pyridine (1 L). The cooling bath was removed, and the reaction was stirred at room temperature for 1 h, after which it was concentrated to provide the crude enone, which was used without any further purification. **29**: LRMS-ESI $[M + Na]^+$ calcd 407.2, found 407.1. **30**: LRMS-ESI $[M + Na]^+$ calcd 305.1, found 305.1.

Sodium borohydride (189 mmol, 7.2 g) was added to a cold (–78 °C) suspension of cerium chloride (94.5 mmol, 25.8 g) and the crude residue from above in ethanol (700 mL) and THF (700 mL). After 90 min of stirring, the solvent was evaporated under reduced pressure, and the residue was redissolved in dichloromethane. The organic layer was sequentially washed with 5% HCl, saturated sodium bicarbonate, and brine, dried (Na_2SO_4), and concentrated. Purification by column chromatography (silica gel, eluting with dichloromethane, 10% ethyl acetate in dichloromethane) provided **31** as a yellow gum (12.63 g, 37% from **28**) and **32** (9.22 g, 34% from **28**) as a white solid. **31**: 1H NMR (300 MHz, $CDCl_3$) δ : 7.89–7.76 (m, 4H), 7.54–7.46 (m, 3H), 5.66 (m, 2H), 5.08 (d, $J = 52.9$ Hz, 1H), 4.90 (d, $J = 12.1$ Hz, 1H), 4.72 (d, $J = 12.2$ Hz, 1H), 4.33 (dd, $J = 3.8, 10.9$ Hz, 1H), 4.20 (m, 1H), 4.14 (dd, $J = 4.7, 11.1$ Hz, 1H), 3.63 (dd, $J = 8.1, 27.3$ Hz, 1H), 2.91–2.82 (m, $J = 4.0$ Hz, 1H), 1.06 (s, 9H). ^{13}C NMR (75 MHz, $CDCl_3$) δ : 178.2, 134.6, 133.2, 128.6, 128.3, 128.3, 128.2, 127.9, 127.7, 127.0, 126.3, 126.2, 125.8, 88.6 (d, $J = 177.8$ Hz, 1C), 74.9 (d, $J = 18.8$ Hz, 1C), 71.7, 67.8 (d, $J = 18.9$, 1C), 63.0, 39.0, 38.9 (d, $J = 6.8$ Hz, 1C), 27.0. ^{19}F NMR (282 MHz, $CDCl_3$) δ : –217.2 (bs, 1F). HRMS-QTOF $[M + Na]^+$ calcd for $C_{23}H_{27}FNao_4$, 409.1791, found 409.1783. LRMS-ESI found 409.1. **32**: 1H NMR (300 MHz, $CDCl_3$) δ : 7.88–7.78 (m, 4H), 7.54–7.43 (m, 3H), 6.25 (d, $J = 10.0$ Hz, 1H), 5.96–5.82 (m, 1H), 5.31 (d, $J = 5.1$ Hz, 2H), 4.82 (d, $J = 12.1$ Hz, 1H), 4.79 (d, partially overlapped, $J = 49.4$ Hz, 1H), 4.72 (d, $J = 12.2$ Hz, 1H), 4.37–4.31 (m, 2H), 3.07 (dd, $J = 1.0, 11.5$ Hz, 1H). ^{13}C NMR (75 MHz, $CDCl_3$) δ : 139.2, 134.7, 133.2, 129.1, 129.0, 128.9, 128.5, 127.9, 127.7, 126.7, 126.3, 126.1, 125.6, 117.8, 89.2 (d, $J = 187.2$ Hz, 1C), 78.0 (d, $J = 19.8$ Hz, 1C), 71.2, 66.4 (d, $J = 18.7$ Hz, 1C). HRMS-QTOF $[M + Na]^+$ calcd for $C_{18}H_{17}FNao_2$, 307.1110, found 307.1107. LRMS-ESI found 307.1.

(2R,3S,4R,5R)-3-Fluoro-2-[(3-N-benzoyl)-thymine-1-yl]-4-(methoxy-2-naphthalene)-5-(pivaloyloxymethyl)-cyclohexene (33 and 34). DIAD (28 mmol, 5.4 mL) was added to a cold (0 °C) solution of **32** (23.3 mmol, 9 g), triphenylphosphine (28 mmol, 7.3 g), and N3 benzoyl thymine (28 mmol, 6.4 g, prepared according to the procedure described in *Chin. Chem. Lett.* **2005**, *16*, 287) in THF (240 mL). The reaction was gradually warmed to room temperature over 1 h and then stirred for another 1 h. The reaction was concentrated under reduced pressure and purified by column chromatography (silica gel, eluting with 10% acetone in hexanes) to provide **33** (11.0 g, 78%) and **34** (2.1 g, 15%). **33**: 1H NMR (300 MHz, $CDCl_3$) δ : 7.94 (d, $J = 7.7$ Hz, 2H, Bz), 7.86–7.62 (m, 3H, Nap), 7.74–7.58 (m, 2H, Ar), 7.56–7.42 (m, 5H, Ar), 6.98 (s, 1H, pyr-H6), 5.88 (d, $J = 9.2$ Hz, 1H, H1), 5.74–5.59 (m, 1H, H6), 5.52–5.37 (m, 1H, H2), 5.02 (dd, $J = 48.8, 7.2$ Hz, 1H, partially overlapped, H3), 4.94 (d, $J = 12.2$ Hz, 1H, CH2), 4.78 (d, $J = 12.4$ Hz, 1H, CH2), 4.16 (dd, $J = 4.5, 11.1$ Hz, 1H, H7), 4.07 (dd, $J = 7.0, 11.1$ Hz, 1H, H7), 3.88 (d, $J = 15.8$ Hz, 1H, H4), 3.04–2.88 (m, 1H, H5), 1.82 (s, 3H, CH3), 1.06 (s, 9H, Piv).

^{13}C NMR (75 MHz, CDCl_3) δ : 178.0, 168.8, 162.6, 149.9, 137.2, 135.1, 134.6, 133.2, 133.1, 131.6, 131.0, 130.5, 129.2, 128.5, 127.9, 127.7, 127.1, 126.4, 126.2, 125.8, 124.2, 111.4, 88.5 (d, J = 185.3 Hz, 1H), 72.9 (d, J = 17.3 Hz, 1C), 72.4, 63.6, 56.7 (d, J = 25.5 Hz, 1C), 41.0 (d, J = 6.0 Hz, 1C), 38.7, 27.1, 12.4. ^{19}F NMR (282 MHz, CDCl_3) δ : -198.2 (m, 1F). HRMS-QTOF $[\text{M} + \text{H}]^+$ calcd for $\text{C}_{35}\text{H}_{36}\text{FN}_2\text{O}_6$ 599.2557, found 599.2551. LRMS-ESI found 599.2. 34: ^1H NMR (300 MHz, CDCl_3) δ : 8.36 (s, 1H), 8.20 (d, J = 7.5 Hz, 2H), 7.90–7.81 (m, 4H), 7.68–7.40 (m, 6H), 5.91–5.89 (m, 1H), 5.88–5.80 (m, 1H), 5.74 (d, J = 11.5 Hz, 1H), 5.12 (dd, J = 4.3, 47.7 Hz, 1H), 4.90 (d, J = 12.1 Hz, 1H), 4.72 (d, J = 12.2 Hz, 1H), 4.34 (dd, J = 4.9, 12.1 Hz, 1H), 4.17 (dd, J = 5.8, 12.2 Hz, 1H), 3.96 (dd, J = 8.1, 26.9 Hz, 1H), 2.95–2.85 (m, 1H), 2.16 (s, 3H), 1.11 (s, 9H). ^{13}C NMR (75 MHz, CDCl_3) δ : 178.3, 165.5, 163.1, 163.0, 161.9, 135.2, 134.4, 133.2, 133.1, 131.5, 130.5, 128.8, 128.3, 128.3, 128.0, 127.6, 126.8, 126.0, 125.9, 125.9, 123.6, 116.4, 87.8 (d, J = 187.7 Hz, 1C), 74.0 (d, J = 19.2 Hz, 1C), 72.4, 72.0 (d, J = 29.6 Hz, 1C), 63.4, 39.2 (d, J = 6.0 Hz, 1C), 38.8, 27.1, 12.2. ^{19}F NMR (282 MHz, CDCl_3) δ : -204.8 (m, 1H). HRMS-QTOF $[\text{M} + \text{Na}]^+$ calcd for $\text{C}_{35}\text{H}_{35}\text{FN}_2\text{NaO}_6$ 621.2377, found 621.2373. LRMS-ESI found 621.2.

(2R,3S,4R,5R)-3-Fluoro-4-hydroxy-5-hydroxymethyl-2-(thymine-1-yl)-cyclohexene (35). DDQ (55.3 mmol, 12.6 g) was added to a biphasic solution of 33 (19.8 mmol, 11.8 g) in dichloromethane (200 mL) and water (10 mL). After stirring at room temperature for 2 h, the reaction was quenched with 10% sodium bisulfate. The resulting mixture was extracted with dichloromethane. The organic layer was then washed with brine then dried (Na_2SO_4) and concentrated. Purification by chromatography (silica gel, eluting with 10% ethyl acetate in dichloromethane) provided 35 (8.4 g, 94%). ^1H NMR (300 MHz, CDCl_3) δ : 7.92 (d, J = 7.7 Hz, 2H), 7.58–7.41 (m, 3H), 7.09 (s, 1H), 5.97 (d, J = 9.8 Hz, 1H), 5.64 (d, J = 10.0 Hz, 1H), 5.47–5.30 (m, 1H), 4.87 (dd, J = 6.2, 48.0 Hz, 1H), 4.25 (dd, J = 4.7, 11.5 Hz, 1H), 4.17 (dd, J = 5.8, 11.7 Hz, 1H), 4.08–3.93 (m, 1H), 3.05 (d, J = 4.7 Hz, 1H), 2.84–2.80 (m, 1H), 1.93 (s, 3H), 1.25 (s, 9H). ^{13}C NMR (75 MHz, CDCl_3) δ : 178.4, 168.8, 162.7, 149.9, 136.9, 135.1, 132.2, 132.0, 131.5, 130.5, 129.2, 128.6, 128.5, 123.3, 123.3, 111.5, 90.5 (J = 180.8 Hz, 1C), 67.2 (J = 18.8 Hz, 1C), 63.9, 55.7 (J = 26.3 Hz, 1C), 41.7 (J = 6.8 Hz, 1C), 38.9, 27.3, 12.5. ^{19}F NMR (282 MHz, CDCl_3) δ : -199.2 (dt, J = 48.2, 16.1, 16.1 Hz, 1H). LRMS-ESI calcd 481.2, found 481.1.

Potassium carbonate (39.8 mmol, 5.5 g) was added to a solution of the benzoyl protected nucleoside (16 mmol, 7.3 g) from above in methanol (400 mL). After stirring at room temperature for 12 h, the reaction was neutralized with acetic acid, and the resulting mixture was concentrated under reduced pressure. Purification by chromatography (silica gel, eluting with 10% MeOH in dichloromethane) provided 35 (3.32 g, 68%). ^1H NMR (300 MHz, CDCl_3) δ : 11.36 (br. s, 1H), 7.38 (s, 1H), 5.88 (d, J = 9.0 Hz, 1H), 5.45 (m, 2H), 5.44–5.30 (m, 2H), 4.82 (dd, J = 7.3, 49.4 Hz, 1H), 4.04 (d, J = 18.5 Hz, 1H), 3.66–3.48 (m, 2H), 2.43 (br. s, 1H), 1.78 (s, 3H). ^{13}C NMR (75 MHz, $\text{DMSO}-d_6$) δ : 163.8, 151.1, 137.7, 132.4, 123.6, 109.4, 90.4 (d, J = 180 Hz, 1C), 66.0 (d, J = 16.5 Hz, 1C), 61.2, 53.2 (d, J = 24.7 Hz, 1C), 46.4 (d, J = 6.6 Hz, 1C), 12.0. ^{19}F NMR (282 MHz, $\text{DMSO}-d_6$) δ : 197.4 (ddd, J = 13.8, 17.2, 49.3 Hz, 1F). HRMS-QTOF $[\text{M} + \text{H}]^+$ calcd for $\text{C}_{12}\text{H}_{15}\text{FN}_2\text{O}_4$ 271.1094, found 271.1089. LRMS-ESI found 271.0.

(2R,3S,4R,5R)-3-Fluoro-4-hydroxy-5-[(4,4'-dimethoxytrityloxy)-methyl]-2-(thymine-1-yl)-cyclohexene (36). DMTrCl (16.1 mmol, 5.4 g) was added to a cold (0 °C) solution of 35 (11.5 mmol, 3.1 g) in pyridine (115 mL). The reaction was then warmed to room temperature, and the reaction was stirred at room temperature for 3 h, after which methanol (10 mL) was added to the reaction. After stirring for 30 min, the reaction was partitioned between ethyl acetate and water. The organic layer was washed with brine, concentrated under reduced pressure, and purified by column chromatography (silica gel, eluting with 2–5% MeOH in dichloromethane) to provide 36 (6.5 g, 98%). ^1H NMR (300 MHz, CDCl_3) δ : 8.71 (s, 1H), 7.45–7.36 (m, 2H), 7.35–7.22 (m, 8H), 6.88–6.81 (m, 4H), 5.92–5.83 (m, 1H), 5.57–5.44 (m, 2H), 4.80 (dd, J = 7.0, 48.6 Hz, 1H), 4.09 (d, J = 18.1 Hz, 1H), 3.79 (s, 6H), 3.46 (dd, J = 4.1, 9.4 Hz, 1H), 3.25 (dd, J = 5.9, 9.3 Hz, 1H), 2.79–2.69 (m, 2H), 1.78 (s, 3H). ^{13}C NMR (75 MHz,

CDCl_3) δ : 163.5, 158.7, 150.9, 144.5, 136.7, 135.6, 135.5, 133.1, 130.1, 128.1, 128.0, 127.1, 123.0, 122.9, 113.3, 111.5, 91.1 (d, J = 180.8 Hz, 1C), 87.0, 68.6 (d, J = 18.0 Hz), 63.9, 55.3, 54.2 (d, J = 25.5 Hz, 1H), 42.9 (d, J = 6.0 Hz, 1C), 12.4. ^{19}F NMR (282 MHz, CDCl_3) δ : -198.4 (dt, J = 14.9, 17.2, 49.3 Hz, 1F). HRMS-QTOF $[\text{M} + \text{Na}]^+$ calcd for $\text{C}_{33}\text{H}_{33}\text{FN}_2\text{NaO}_6$ 595.2220, found 595.2207. LRMS-ESI found 595.2.

(2R,3S,4R,5R)-4-[2-Cyanoethoxy(diisopropylamino)-phosphinoxy]-5-[(4,4'-dimethoxytrityloxy)-methyl]-3-fluoro-2-(thymine-1-yl)-cyclohexene (37). To a solution of 36 (5.6 mmol, 3.2 g) and tetrazole (4.5 mmol, 0.31 g) in DMF (29 mL) at 0 °C were added 1-methyl imidazole (1.4 mmol, 0.11 mL) and 2-cyanoethyltetraisopropyl phosphorodiamidite (8.4 mmol, 2.7 mL). The reaction was warmed to room temperature and stirred for 2 h. The reaction was quenched with saturated sodium bicarbonate extracted with ethyl acetate. The organic layer was washed with brine, dried (Na_2SO_4), and concentrated under reduced pressure. Purification by column chromatography (silica gel, eluting with 33% ethyl acetate in hexanes) provided 37 (3.88 g, 90%). ^{31}P NMR (121 MHz, CDCl_3) δ : 151.6 (d, J = 18.3 Hz, 1P), 150.9 (d, J = 9.1 Hz, 1P). LRMS-ESI $[\text{M} + \text{H}]^+$ calcd 773.3, found 773.3.

(2R,3S,4R,5R)-4-(tert-Butyldimethylsilyloxy)-5-[(4,4'-dimethoxytrityloxy)-methyl]-3-fluoro-2-(thymine-1-yl)-cyclohexene (38). TBSCI (16.9 mmol, 2.9 g) was added to a cold (0 °C) solution of 36 (6.75 mmol, 3.9 g) and imidazole (43.8 mmol, 3.0 g) in DMF (60 mL). After the addition, the ice bath was removed, and the reaction was warmed to room temperature and stirred for 16 h. The reaction was quenched with saturated sodium bicarbonate and extracted with diethyl ether. The organic layer was then washed with brine, dried (Na_2SO_4), and concentrated under reduced pressure. Purification by column chromatography (silica gel, eluting with 1% methanol in dichloromethane) provided 38 (3.51 g, 76%, contaminated with trace DMF). ^1H NMR (300 MHz, CDCl_3) δ : 8.53 (s, 1H), 7.39–7.31 (m, 2H), 7.29–7.12 (m, 8H), 6.77 (d, J = 8.9 Hz, 4H), 5.75–5.56 (m, 1H), 5.45–5.36 (m, 2H), 4.41 (dd, J = 8.9, 49.4 Hz, 1H), 4.14 (d, J = 12.2 Hz, 1H), 3.72 (s, 6H), 3.26 (dd, J = 4.9, 9.6 Hz, 1H), 3.06 (dd, J = 7.5, 9.8 Hz, 1H), 2.65–2.58 (m, 1H), 1.73 (s, 3H), 0.82 (s, 9H), 0.04 (s, 3H), 0.00 (s, 3H). ^{13}C NMR (75 MHz, CDCl_3) δ : 163.7, 158.7, 150.8, 144.6, 137.3, 135.7, 135.6, 130.5, 130.1, 128.2, 127.9, 127.0, 124.9, 124.8, 113.2, 111.2, 90.1 (d, J = 186.0 Hz, 1C), 86.8, 69.6 (d, J = 15.8 Hz, 1C), 63.7, 55.2, 46.7 (d, J = 7.5 Hz, 1C), 31.4, 25.7, 18.1, 12.4, -4.7, -4.9. ^{19}F NMR (282 MHz, CDCl_3) δ : -196.8 (d, J = 49.3 Hz, 1F). HRMS-QTOF $[\text{M} + \text{Na}]^+$ calcd for $\text{C}_{39}\text{H}_{47}\text{FN}_2\text{NaO}_6\text{Si}$ 709.3085, found 709.3074. LRMS-ESI found 709.3.

(2R,3S,4R,5R)-2-[(4-N-Benzoyl-5-methyl)-cytosin-1-yl]-4-(tert-butylidimethylsilyloxy)-5-[(4,4'-dimethoxytrityloxy)-methyl]-3-fluoro-cyclohexene (39). POCl_3 (40 mmol, 3.66 mL) was added to a cold (0 °C) suspension of 1,2,4-triazole (160 mmol, 11 g) in CH_3CN (40 mL) at 0 °C. The mixture was stirred at 0 °C for 15 min, Et_3N (200.0 mmol, 28.0 mL) was added, and the stirring was continued for another 30 min at 0 °C. A solution of 38 (5.0 mmol, 3.43 g) was added via a cannula, and the reaction was warmed to room temperature and stirred for 2 h. The reaction was concentrated under reduced pressure and suspended in ethyl acetate. The organic layer was then washed with water and brine, dried (Na_2SO_4), and concentrated under reduced pressure to provide the crude triazolide, which was used without any further purification.

The residue from above was dissolved in a mixture of 1,4-dioxane (50 mL) and aqueous ammonia (27 mL of a 32% aqueous solution), and the reaction was aged at room temperature for 16 h. The reaction was then partitioned between ethyl acetate and water, and the organic layer was washed with brine, dried (Na_2SO_4), and concentrated under reduced pressure. Purification by column chromatography (silica gel, eluting with 2% methanol in dichloromethane) provided the cytosine nucleoside (3.0 g). ^1H NMR (300 MHz, CDCl_3) δ : 7.38 (d, J = 7.2 Hz, 2H), 7.31–7.22 (m, 7H), 6.85 (s, 1H), 6.79 (d, J = 8.7 Hz, 4H), 5.66 (d, J = 9.2 Hz, 1H), 5.46 (d, J = 8.1 Hz, 1H), 5.40–5.26 (m, 1H), 4.62 (dd, J = 6.8, 49.2 Hz, 1H), 4.17 (d, J = 15.8 Hz, 1H), 3.75 (s, 6H), 3.26 (dd, J = 4.6, 9.3 Hz, 1H), 3.15 (d, J = 7.2 Hz, 1H), 2.64–2.58 (m, 1H), 2.00 (br. s, 1H), 1.71 (s, 3H), 0.83 (s, 9H), 0.05 (s, 4H), 0.00 (s,

3H). ^{13}C NMR (75 MHz, CDCl_3) δ : 165.6, 158.6, 156.5, 144.8, 140.6, 135.9, 135.8, 130.2, 130.1, 128.2, 127.9, 126.9, 125.3, 113.2, 101.9, 90.0 (d, $J = 182.3$ Hz, 1C), 86.5, 69.0 (d, $J = 16.5$ Hz, 1C), 63.7, 55.3, 45.7 (d, $J = 5.3$ Hz, 1C), 30.9, 25.8, 18.1, 13.0, -4.5, -4.9. ^{19}F NMR (282 MHz, CDCl_3) δ : -197.6 (d, $J = 49.3$ Hz, 1F). LRMS-ESI calcd 686.3, found 686.3.

Benzoic anhydride (5.51 mmol, 1.25 g) was added to a cold (0 °C) solution of the cytosine nucleoside from above (4.24 mmol, 2.90 g) in DMF (40 mL). The reaction was warmed to room temperature and stirred for 36 h. The reaction was quenched with saturated sodium bicarbonate solution and extracted with ethyl acetate. The organic layer was then washed with brine, dried (Na_2SO_4), and concentrated under reduced pressure. Purification by column chromatography (silica gel, eluting with 10% ethyl acetate in hexanes) provided **39** (3.02 g, 78% from **38**). ^1H NMR (300 MHz, CDCl_3) δ : 8.24 (d, $J = 7.2$ Hz, 2H), 7.46–7.32 (m, 5H), 7.29–7.17 (m, 7H), 6.90 (s, 1H), 6.77 (d, $J = 8.9$ Hz, 4H), 5.66 (d, $J = 8.7$ Hz, 1H), 5.51–5.35 (m, 2H), 4.48 (d, $J = 49.5$, 8.1 Hz, 1H), 4.15 (d, $J = 12.2$ Hz, 1H), 3.72 (s, 6H), 3.28 (dd, $J = 4.4$, 9.7 Hz, 1H), 3.08 (d, $J = 7.3$ Hz, 1H), 2.60–2.53 (m, 1H), 0.82 (s, 9H), 0.07 (s, 3H), 0.05 (s, 3H). ^{13}C NMR (75 MHz, CDCl_3) δ : 179.6, 159.8, 158.7, 148.7, 144.6, 138.7, 137.3, 135.7, 135.6, 132.4, 130.6, 130.1, 129.9, 128.2, 128.1, 128.0, 127.1, 124.7, 124.6, 113.2, 112.3, 90.0 (d, $J = 185.3$ Hz, 1C), 86.8, 69.5 (d, $J = 15.8$ Hz, 1C), 63.7, 55.3, 46.7 (d, $J = 6.8$, Hz, 1C), 25.7, 18.1, 13.5, -4.6, -4.9. ^{19}F NMR (282 MHz, CDCl_3) δ : -196.7 (d, $J = 50.5$ Hz, 1F). HRMS-QTOF $[M + H]^+$ calcd for $\text{C}_{46}\text{H}_{53}\text{FN}_3\text{O}_6\text{Si}$ 790.3688, found 790.3681. LRMS-ESI found 821.3.

(2R,3S,4R,5R)-2-[(4-N-Benzoyl-5-methyl)-cytosin-1-yl]-5-[(4,4'-dimethoxytrityloxy)-methyl]-3-fluoro-4-hydroxy-cyclohexene (40). TBAF (4.6 mmol, 4.6 mL of 1.0 M THF solution) was added to a cold (0 °C) solution of **39** (3.8 mmol, 3.0 g) in THF (40 mL). The reaction was warmed to room temperature and stirred for 70 min. The reaction was partitioned between ethyl acetate and water, and the organic layer was washed with brine, dried (Na_2SO_4), and concentrated under reduced pressure. Purification by column chromatography (silica gel, eluting with 33% ethyl acetate in hexanes) provided **40** (2.4 g, 93%). ^1H NMR (300 MHz, CDCl_3) δ : 8.31 (d, $J = 7.3$ Hz, 2H), 7.60–7.49 (m, 1H), 7.47–7.39 (m, 4H), 7.36–7.25 (m, 7H), 7.08 (s, 1H), 6.85 (d, $J = 8.9$ Hz, 4H), 5.91 (d, $J = 10.2$ Hz, 1H), 5.61–5.47 (m, 2H), 4.83 (dd, $J = 5.7$, 48.8 Hz, 1H), 4.19–4.02 (m, 1H), 3.79 (s, 6H), 3.48 (dd, $J = 4.1$, 9.3 Hz, 1H), 3.28 (dd, $J = 5.7$, 10.4 Hz, 1H). ^{13}C NMR (75 MHz, CDCl_3) δ : 179.6, 159.6, 158.7, 148.7, 144.5, 138.0, 137.1, 135.6, 135.5, 133.5, 132.5, 130.1, 129.9, 128.1, 128.0, 127.1, 122.7, 122.6, 113.3, 112.5, 91.0 (d, $J = 180$ Hz, 1C), 87.0, 68.5 (d, $J = 17.3$, 1C), 63.8, 55.3, 55.2, 54.8, 42.8 (d, $J = 6.8$ Hz, 1C), 13.5. ^{19}F NMR (282 MHz, CDCl_3) δ : -198.4 (dt, $J = 14.9$, 16.1, 49.3 Hz, 1F). HRMS-QTOF $[M + H]^+$ calcd for $\text{C}_{40}\text{H}_{39}\text{FN}_3\text{O}_6$ 676.2823, found 676.2816. LRMS-ESI found 698.2.

(2R,3S,4R,5R)-2-[(4-N-Benzoyl-5-methyl)-cytosin-1-yl]4-[2-cyanoethoxy(diisopropylamino)-phosphinoxy]-5-[(4,4'-dimethoxytrityloxy)-methyl]-3-fluoro-cyclohexene (41). To a solution of **40** (3.5 mmol, 2.35 g) and tetrazole (2.8 mmol, 0.2 g) in DMF (18 mL) at 0 °C were added 1-methyl imidazole (0.87 mmol, 0.069 mL) and 2-cyanoethyltetraisopropyl phosphorodiamidite (5.2 mmol, 1.67 mL). The reaction was warmed to room temperature and stirred for 5 h. The reaction was diluted with ethyl acetate, and the organic layer was washed with brine, dried (Na_2SO_4), and concentrated under reduced pressure. Purification by column chromatography (silica gel, eluting with 33% ethyl acetate in hexanes) provided **41** (2.6 g, 95%). ^{31}P NMR (121 MHz, CDCl_3) δ : 151.6 (d, $J = 18.3$ Hz, 1P), 150.8 (d, $J = 11.0$ Hz, 1P). LRMS-ESI calcd 876.4, found 876.3.

Oligonucleotide Synthesis and Purification. Oligonucleotides 1–21 (Supporting Information) were synthesized at 2 μmol scale using T-CPG or UnyLinker support, 0.1 M solutions of all phosphoramidites in acetonitrile, and standard oxidizing and capping reagents. An extended coupling time of 5 min was used for incorporation of the modified analogues. Oligonucleotides **A1** and **A2** were synthesized at 40 μmol scale using UnyLinker PS200 universal support, 0.2 M phenylacetyldisulfide (PADS) in 1:1 3-picoline/acetonitrile as a sulfur-transfer reagent, 20% *tert*-butylhy-

droperoxide in wet acetonitrile as oxidizer, and 0.7 M dicyanoimidazole in acetonitrile as the activator. All phosphoramidites were used at 0.1 M concentration in acetonitrile. For each of the modified analogues 4-fold excess of amidite was delivered with a 12 min coupling time. The 5'-end dimethoxytrityl group was left on to facilitate purification. Postsynthetically, all oligonucleotides were treated with 1:1 triethylamine/acetonitrile to afford removal of the cyanoethyl protecting group from the phosphate/phosphorothioate bridges. Subsequently, oligonucleotides were treated with conc aq NH_4OH at 55 °C for 9–12 h to cleave from support, remove heterocyclic protecting groups, and hydrolyze the UnyLinker moiety (**A1** and **A2**). Oligonucleotides 1–21 were purified by ion-exchange chromatography using a gradient of NaBr across a column packed with Source 30Q resin. Pure fractions were desalted using C18 SepPak cartridges. Oligonucleotides **A1** and **A2** were purified by ion-exchange chromatography using a gradient of NaBr across Source 30Q resin, with the 5'-DMT group being removed during purification using 6% (v/v) aq dichloroacetic acid. Pure fractions were desalted by binding to a C18 reverse-phase column and eluting with 50% (v/v) acetonitrile in water. Purity and mass of oligonucleotides was determined using ion-pair LC–MS.

T_m Measurements. For the T_m experiments, oligonucleotides were prepared at a concentration of 8 μM in a buffer of 100 mM Na^+ , 10 mM phosphate, 0.1 mM EDTA, pH 7. Concentration of oligos was determined at 85 °C. The oligo concentration was 4 μM with mixing of equal volumes of test oligo and match or mismatch RNA strand. Oligos were hybridized with the complementary or mismatch RNA strand by heating the duplex to 90 °C for 5 min and allowed to cool at room temperature. Using the spectrophotometer, T_m measurements were taken by heating the duplex solution at a rate of 0.5 °C/min in cuvette starting at 15 °C and heating to 85 °C. T_m values were determined using Vant Hoff calculations (A_{260} vs temperature curve) using non-self-complementary sequences where the minimum absorbance that relates to the duplex and the maximum absorbance that relates to the nonduplex single strand are manually integrated into the program.

■ ASSOCIATED CONTENT

📄 Supporting Information

^1H , ^{13}C , and ^{19}F NMR spectra for all new compounds; ^{31}P NMR spectra for all phosphoramidites; analytical data for oligonucleotides; CIF and RTF files for crystal structures. This material is available free of charge via the Internet at <http://pubs.acs.org>.

■ AUTHOR INFORMATION

Corresponding Author

*E-mail: pseth@isisph.com.

Notes

The authors declare no competing financial interest.

■ ACKNOWLEDGMENTS

The authors thank Dr. Hans Gaus, Andres Berdeja and Dr. Karsten Schmidt for assistance with analytical measurements and Dr. T. P. Prakash for assistance with oligonucleotide synthesis.

■ REFERENCES

- (1) Monia, B. P.; Lesnik, E. A.; Gonzalez, C.; Lima, W. F.; McGee, D.; Guinasso, C. J.; Kawasaki, A. M.; Cook, P. D.; Freier, S. M. *J. Biol. Chem.* **1993**, *268*, 14514.
- (2) Pieken, W.; Olsen, D.; Benseler, F.; Aurup, H.; Eckstein, F. *Science* **1991**, *253*, 314.
- (3) Rigo, F.; Hua, Y.; Chun, S. J.; Prakash, T. P.; Krainer, A. R.; Bennett, C. F. *Nat. Chem. Biol.* **2012**, DOI: 10.1038/nchembio.939.

- (4) Davis, S.; Propp, S.; Freier, S. M.; Jones, L. E.; Serra, M. J.; Kinberger, G.; Bhat, B.; Swayze, E. E.; Bennett, C. F.; Esau, C. *Nucleic Acids Res.* **2009**, *37*, 70.
- (5) Allerson, C. R.; Sioufi, N.; Jarres, R.; Prakash, T. P.; Naik, N.; Berdeja, A.; Wanders, L.; Griffey, R. H.; Swayze, E. E.; Bhat, B. *J. Med. Chem.* **2005**, *48*, 901.
- (6) Manoharan, M.; Akinc, A.; Pandey, R. K.; Qin, J.; Hadwiger, P.; John, M.; Mills, K.; Charisse, K.; Maier, M. A.; Nechev, L.; Greene, E. M.; Pallan, P. S.; Rozners, E.; Rajeev, K. G.; Egli, M. *Angew. Chem., Int. Ed.* **2011**, *50*, 2284.
- (7) Ng, E. W.; Shima, D. T.; Calias, P.; Cunningham, E. T., Jr.; Guyer, D. R.; Adamis, A. P. *Nat. Rev. Drug Discovery* **2006**, *5*, 123.
- (8) Williams, D. M.; Benseler, F.; Eckstein, F. *Biochemistry* **1991**, *30*, 4001.
- (9) Kawasaki, A. M.; Casper, M. D.; Freier, S. M.; Lesnik, E. A.; Zounes, M. C.; Cummins, L. L.; Gonzalez, C.; Cook, P. D. *J. Med. Chem.* **1993**, *36*, 831.
- (10) Fazakerley, G. V.; Uesugi, S.; Izumi, A.; Ikehara, M.; Guschlbauer, W. *FEBS Lett.* **1985**, *182*, 365.
- (11) Pallan, P. S.; Greene, E. M.; Jicman, P. A.; Pandey, R. K.; Manoharan, M.; Rozners, E.; Egli, M. *Nucleic Acids Res.* **2011**, *39*, 3482.
- (12) Damha, M. J.; Wilds, C. J.; Noronha, A.; Brukner, I.; Borkow, G.; Arion, D.; Parniak, M. A. *J. Am. Chem. Soc.* **1998**, *120*, 12976.
- (13) Wilds, C. J.; Damha, M. J. *Nucleic Acids Res.* **2000**, *28*, 3625.
- (14) Berger, I.; Tereshko, V.; Ikeda, H.; Marquez, V. E.; Egli, M. *Nucleic Acids Res.* **1998**, *26*, 2473.
- (15) Minasov, G.; Teplova, M.; Nielsen, P.; Wengel, J.; Egli, M. *Biochemistry* **2000**, *39*, 3525.
- (16) Anzahae, M. Y.; Watts, J. K.; Alla, N. R.; Nicholson, A. W.; Damha, M. J. *J. Am. Chem. Soc.* **2011**, *133*, 728.
- (17) Egli, M.; Pallan, P. S.; Allerson, C. R.; Prakash, T. P.; Berdeja, A.; Yu, J.; Lee, S.; Watt, A.; Gaus, H.; Bhat, B.; Swayze, E. E.; Seth, P. P. *J. Am. Chem. Soc.* **2011**, *133*, 16642.
- (18) Pallan, P. S.; Yu, J.; Allerson, C. R.; Swayze, E. E.; Seth, P.; Egli, M. *Biochemistry* **2011**, *51*, 7.
- (19) Herdewijn, P. *Chem. Biodiversity* **2010**, *7*, 1.
- (20) Lescrinier, E.; Esnouf, R.; Schraml, J.; Busson, R.; Heus, H.; Hilbers, C.; Herdewijn, P. *Chem. Biol.* **2000**, *7*, 719.
- (21) Verbeure, B.; Lescrinier, E.; Wang, J.; Herdewijn, P. *Nucleic Acids Res.* **2001**, *29*, 4941.
- (22) Herdewijn, P.; De Clercq, E. *Bioorg. Med. Chem. Lett.* **2001**, *11*, 1591.
- (23) Wang, J.; Verbeure, B.; Luyten, I.; Lescrinier, E.; Froeyen, M.; Hendrix, C.; Rosemeyer, H.; Seela, F.; Van Aerschot, A.; Herdewijn, P. *J. Am. Chem. Soc.* **2000**, *122*, 8595.
- (24) Wang, J.; Froeyen, M.; Hendrix, C.; Andrei, G.; Snoeck, R.; De Clercq, E.; Herdewijn, P. *J. Med. Chem.* **2000**, *43*, 736.
- (25) Robeyns, K.; Herdewijn, P.; Van Meervelt, L. *J. Am. Chem. Soc.* **2008**, *130*, 1979.
- (26) Robeyns, K.; Herdewijn, P.; Van Meervelt, L. *Nucleic Acids Res.* **2008**, *36*, 1407.
- (27) Robeyns, K.; Herdewijn, P.; Van Meervelt, L. *Artif. DNA: PNA & XNA* **2010**, *1*, 2.
- (28) Nauwelaerts, K.; Fisher, M.; Froeyen, M.; Lescrinier, E.; Van Aerschot, A.; Xu, D.; DeLong, R.; Kang, H.; Juliano, R. L.; Herdewijn, P. *J. Am. Chem. Soc.* **2007**, *129*, 9340.
- (29) Seth, P. P.; Allerson, C. R.; Berdeja, A.; Siwkowski, A.; Pallan, P. S.; Gaus, H.; Prakash, T. P.; Watt, A. T.; Egli, M.; Swayze, E. E. *J. Am. Chem. Soc.* **2010**, *132*, 14942.
- (30) Cerritelli, S. M.; Crouch, R. J. *FEBS J.* **2009**, *276*, 1494.
- (31) Wu, H.; Lima, W. F.; Zhang, H.; Fan, A.; Sun, H.; Croke, S. T. *J. Biol. Chem.* **2004**, *279*, 17181.
- (32) Liu, J.; Carmell, M. A.; Rivas, F. V.; Marsden, C. G.; Thomson, J. M.; Song, J. J.; Hammond, S. M.; Joshua-Tor, L.; Hannon, G. J. *Science* **2004**, *305*, 1437.
- (33) Gu, P.; Schepers, G.; Griebel, C.; Rozenski, J.; Gais, H. J.; Herdewijn, P.; Van Aerschot, A. *Nucleosides, Nucleotides Nucleic Acids* **2005**, *24*, 993.
- (34) Wang, J.; Vina, D.; Busson, R.; Herdewijn, P. *J. Org. Chem.* **2003**, *68*, 4499.
- (35) Wang, J.; Morral, J.; Hendrix, C.; Herdewijn, P. *J. Org. Chem.* **2001**, *66*, 8478.
- (36) Horvath, A.; Ruttens, B.; Herdewijn, P. *Tetrahedron Lett.* **2007**, *48*, 3621.
- (37) Jung, M. E.; Choe, S. W. T. *J. Org. Chem.* **1995**, *60*, 3280.
- (38) Xia, J.; Abbas, S. A.; Locke, R. D.; Piskorz, C. F.; Alderfer, J. L.; Matta, K. L. *Tetrahedron Lett.* **2000**, *41*, 169.
- (39) Seth, P. P.; Vasquez, G.; Allerson, C. A.; Berdeja, A.; Gaus, H.; Kinberger, G. A.; Prakash, T. P.; Migawa, M. T.; Bhat, B.; Swayze, E. E. *J. Org. Chem.* **2010**, *75*, 1569.
- (40) Mancuso, A. J.; Huang, S.-L.; Swern, D. *J. Org. Chem.* **1978**, *43*, 2480.
- (41) Takamatsu, S.; Katayama, S.; Hirose, N.; De Cock, E.; Schelkens, G.; Demillequand, M.; Brepoels, J.; Izawa, K. *Nucleosides, Nucleotides Nucleic Acids* **2002**, *21*, 849.
- (42) Bechor, Y.; Albeck, A. *Tetrahedron* **2008**, *64*, 2080.
- (43) Takahashi, H.; Ikegami, S. *Molecules* **2005**, *10*, 901.
- (44) It should be noted that this elimination was not observed when the primary hydroxyl group was protected as the Nap ether.
- (45) Luche, J. L. *J. Am. Chem. Soc.* **1978**, *100*, 2226.
- (46) Busson, R.; Kerremans, L.; Aerschot, A. V.; Peeters, M.; Bleton, N.; Herdewijn, P. *Nucleosides, Nucleotides Nucleic Acids* **1999**, *18*, 1079.
- (47) Seth, P. P.; Allerson, C. R.; Østergaard, M. E.; Swayze, E. E. *Bioorg. Med. Chem. Lett.* **2012**, *22*, 296.
- (48) Seth, P. P.; Yu, J.; Allerson, C. R.; Berdeja, A.; Swayze, E. E. *Bioorg. Med. Chem. Lett.* **2011**, *21*, 1122.
- (49) Seth, P. P.; Allerson, C. A.; Østergaard, M. E.; Swayze, E. E. *Bioorg. Med. Chem. Lett.* **2011**, *21*, 4690.
- (50) Seth, P. P.; Allerson, C. R.; Siwkowski, A.; Vasquez, G.; Berdeja, A.; Migawa, M. T.; Gaus, H.; Prakash, T. P.; Bhat, B.; Swayze, E. E. *J. Med. Chem.* **2010**, *53*, 8309.
- (51) AbdurRahman, S. M.; Seki, S.; Obika, S.; Yoshikawa, H.; Miyashita, K.; Imanishi, T. *J. Am. Chem. Soc.* **2008**, *130*, 4886.
- (52) Mori, K.; Kodama, T.; Baba, T.; Obika, S. *Org. Biomol. Chem.* **2011**, *9*, 5272.
- (53) Obika, S.; Nanbu, D.; Hari, Y.; Andoh, J.-I.; Morio, K.-I.; Doi, T.; Imanishi, T. *Tetrahedron Lett.* **1998**, *39*, 5401.
- (54) Petersen, M.; Bondensgaard, K.; Wengel, J.; Jacobsen, J. P. *J. Am. Chem. Soc.* **2002**, *124*, 5974.
- (55) Teplova, M.; Wallace, S. T.; Tereshko, V.; Minasov, G.; Symons, A. M.; Cook, P. D.; Manoharan, M.; Egli, M. *Proc. Nat. Acad. Sci. U.S.A.* **1999**, *96*, 14240.
- (56) Seth, P. P.; Siwkowski, A.; Allerson, C. R.; Vasquez, G.; Lee, S.; Prakash, T. P.; Wancewicz, E. V.; Wittchell, D.; Swayze, E. E. *J. Med. Chem.* **2009**, *52*, 10.
- (57) Prakash, T. P.; Siwkowski, A.; Allerson, C. R.; Migawa, M. T.; Lee, S.; Gaus, H. J.; Black, C.; Seth, P. P.; Swayze, E. E.; Bhat, B. *J. Med. Chem.* **2010**, *53*, 1636.
- (58) Pinheiro, V. B.; Taylor, A. I.; Cozens, C.; Abramov, M.; Renders, M.; Zhang, S.; Chaput, J. C.; Wengel, J.; Peak-Chew, S.-Y.; McLaughlin, S. H.; Herdewijn, P.; Holliger, P. *Science* **2012**, *336*, 341.